FLOW RATE MEASURMENT OF *IN SITU* PERFUSION THROUGH THE AQUEOUS HUMOR OUTFLOW NETWORK

by

NOEL ORTIZ LAWRENCE

Presented to the Faculty of the Graduate School of

The University of Texas at Arlington in Partial Fulfillment

of the Requirements

for the Degree of

MASTER OF SCIENCE IN BIOMEDICAL ENGINEERING

THE UNIVERSITY OF TEXAS AT ARLINGTON

AUGUST 2006

ACKNOWLEDGEMENTS

The author appreciatively thanks Drs. Chuong, Pang, and Zuzak for sitting on the committee and for the opportunity to work on the project. Thanks are also due to Peggy E. Hellberg for her organ culture expertise and assistance. Funding was provided by Alcon Laboratories, Inc.

July 20, 2006

ABSTRACT

FLOW RATE MEASURMENT OF *IN SITU* PERFUSION THROUGH THE AQUEOUS HUMOR OUTFLOW NETWORK

Publication No. _____

Noel Ortiz Lawrence, M.S.

The University of Texas at Arlington, 2006

Supervising Professor: Dr. C. J. Chuong

A system was developed to measure the instantaneous perfusate flow rate through the aqueous humor (AH) outflow network of a human eye, while under constant pressure. The system monitors real-time weight changes of the perfusate reservoir, associated with perfusate flow through the AH outflow network. The recorded weight changes of the reservoir are used as an indicator of flow rates. Methods to determine time and flow rate resolution and to control for evaporation were also developed.

The system is capable of measuring flow on a μL/min scale; determined by the following model, which includes a range of uncertainty (implies flow rate resolution) and time resolution.

$$Q = (\Delta W/\Delta t - E) / \rho \pm 0.0003 / (\Delta t * \rho)$$

Where:

Q – flow rate (mL/min)
$\Delta W/\Delta t$ – is the weight change over time as recorded by the balance (g/min); Δt is the time resolution
E – rate of evaporation (g/min); empirically found and assumed to be constant
ρ – density of the perfusate (g/mL); a density value of 1g/mL is used
0.0003 – nonlinearity of balance (g)

The system was set up using a porcine eye specimen; the cornea was punctured to determine the systems ability to monitor the increase in flow rate. A second test was conducted, in which an undisclosed compound was perfused through the porcine AH outflow network. The system was able to monitor the flow rate changes due to the corneal puncture and added compound.

TABLE OF CONTENTS

LIST OF FIGURES

CHAPTER 1

INTRODUCTION

1.1 Background

The human eye produces aqueous humor (AH) at a documented rate of 2.44 µL/min [5], with daytime peaks of 4.26 µL/min and nighttime valleys of 1.08 µL/min [6]. AH is produced actively by ciliary epithelium in the posterior chamber of the eye (Figure 1.1) and flows through the pupil to the anterior chamber; here it provides nutrients to the cornea, removes cell waste products, and maintains the cornea shape[1]. AH normally drains to the venous system via an outflow network that includes the trabecular meshwork (a network of ECM and trabecular cells located where the iris and cornea meet), Schlemm's canal, and episcleral veins [1].

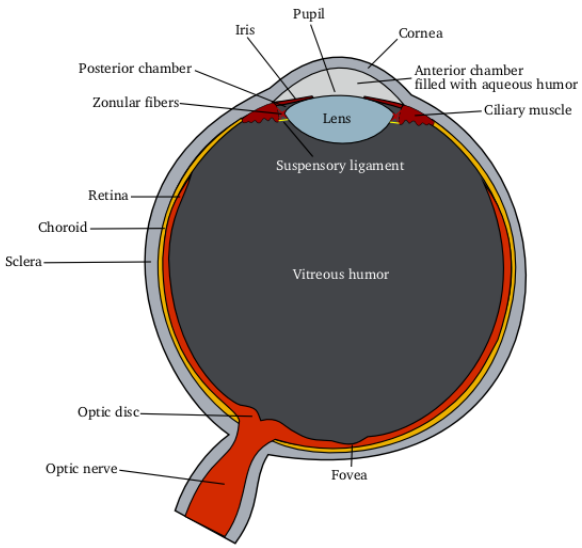

Figure 1.1 Schematic of Human Eye (from reference 9)

The intraocular pressure (IOP) of the eye is maintained by the hydrodynamic resistance of the AH outflow network. This resistance is significant enough to cause a pressure drop of 6 mmHg across a distance of less than 1 mm. The major contributor to this hydrodynamic resistance is the region along the inner wall of the Schlemm's canal (the trabecular tissues). An increase in the AH outflow resistance causes an elevated IOP, which can ultimately lead to glaucoma. Glaucomatous eyes can experience a pressure drop as high as 40 mmHg across the mentioned outflow pathway. [7]

Glaucoma is a disease of the eye, which ultimately causes blindness by optic nerve damage, usually caused by increased (IOP). Primary open angle glaucoma (POAG) is the most common form of glaucoma. Primary refers the class of glaucoma with no known etiology; as opposed to secondary glaucoma, which is caused by a previous injury or illness [1]. Open angle refers to the iridial angle (between the iris and the cornea); an open angle provides an opportunity for the AH to leave the anterior chamber. When this angle is zero, as in acute angle-closure glaucoma, the AH outflow pathway is blocked by the iris.

The illustration below (Figure 1.2) shows a cross section the AH outflow network. It includes the trabecular meshwork, Schlemm's canal (sinus venous sclera), and an open iridial angle.

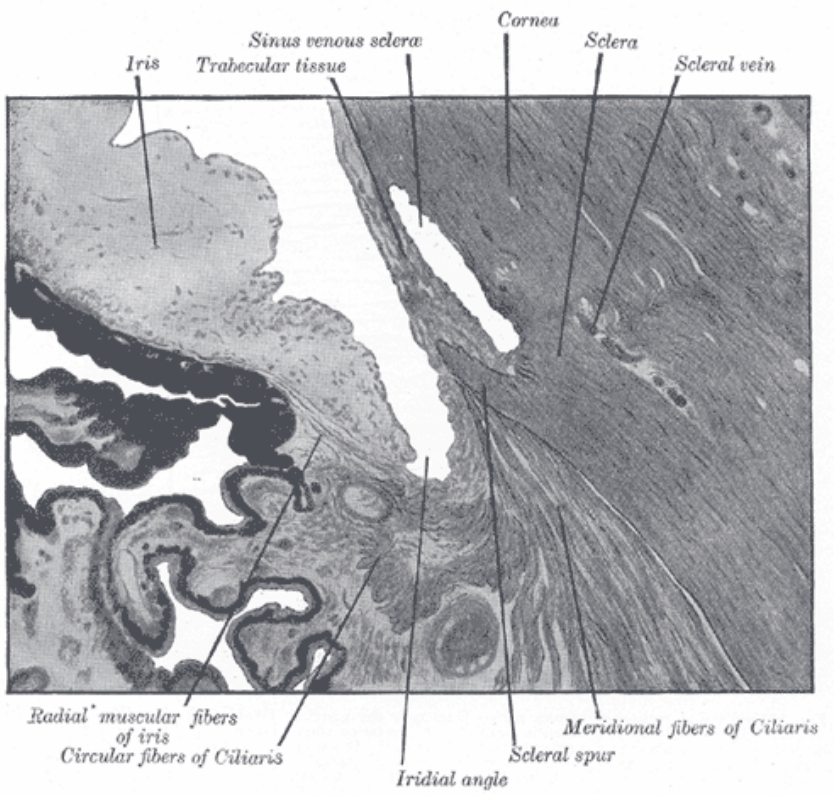

Figure 1.2: Aqueous Humor Outflow Network (from reference 9).

Conventional treatments for primary open-angle glaucoma aim to reduce AH production, and include: α-adrenergic receptor agonists, β-adrenergic receptor antagonists, and carbonic anhydrase inhibitors [2, 3]. An alternate technique is to increase/restore the AH outflow through the normal outflow pathway, as by muscarinic acetylcholine receptor agonists [2]. This technique is more appealing as it allows for natural levels of aqueous humor production [3].

1.2 Purpose

Currently, *in situ* studies of the AH outflow network are conducted using a modified Petri dish, which holds the anterior portion of an eyeball bisected along the frontal plane (see figure 1.3).

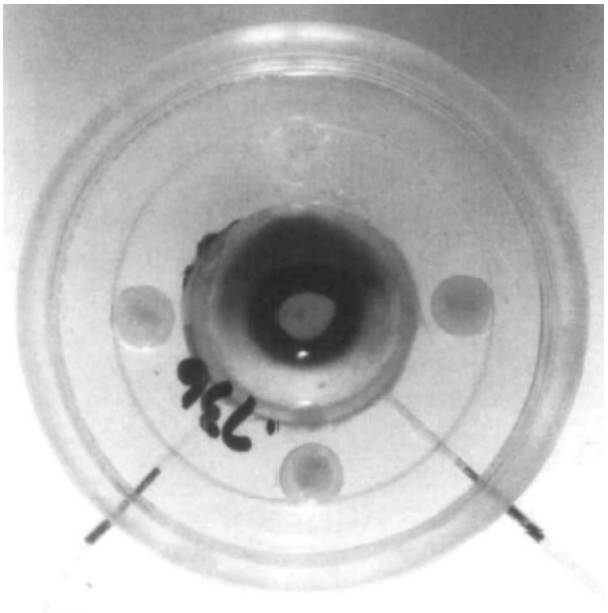

Figure 1.3 Modified Petri Dish (from reference 5).

The vitreous humor and lens are removed and the aqueous veins are severed. This setup allows for perfusate (media that acts as an AH analog) to flow into the eye chamber, via one of the two cannulae, and drain into the dish, via the AH outflow network (see figure 1.4). The other cannula is used to measure intraocular pressure and drain/replace the perfusate when necessary. [5] The Petri dish is placed in an incubator at 37 ^{o}C.

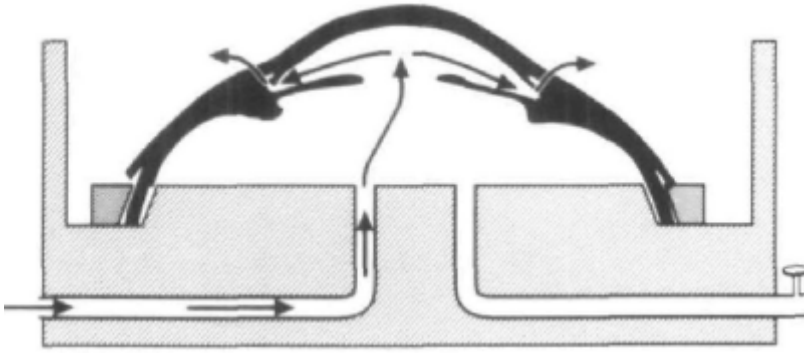

Figure 1.4 Schematic of Modified Petri Dish (from reference 6).

Perfusate is infused from a reservoir via plastic tubing (ID = 0.03") by one of two methods: a micro-infusion pump [5], which provides a constant flow rate; or the utilization of hydrostatic pressure, from an elevated reservoir (Erlenmeyer flask) in the incubator. The latter method provides constant pressure, but the instantaneous flow rate is unknown. The purpose of this project was to design a system capable of measuring the flow rate, with 0.1 μL/min resolution, through the AH outflow network under constant pressure.

1.3 Design Parameters

The required specifications for the design of the system are as follows. The system must be capable of measuring 0-10 μL/min, with a 0.1 μL/min flow rate resolution, and a time resolution less than one hour. In order to maintain constant pressure at the eye, the system must be non-intrusive where pressure is concerned. It is also desirable to simultaneously monitor the flow rate through multiple eyes.

1.4 Solution

The implemented solution is to monitor the weight of the perfusate reservoir, outside the incubator, and correlate weight changes to flow rates.

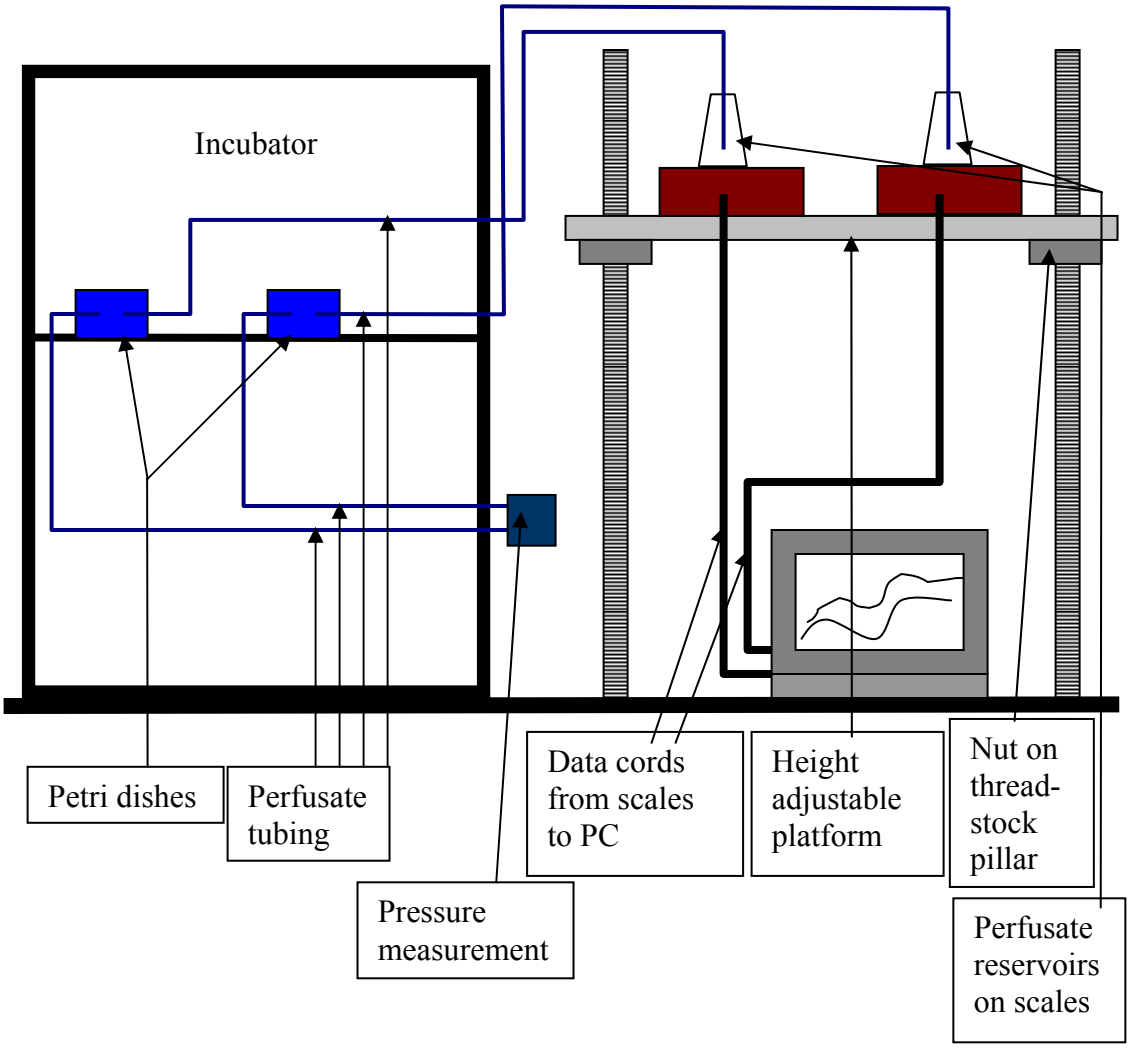

Figure 1.5: Schematic of System

The developed system, depicted in figure 1.5, weighs the perfusate reservoir in real time using a lab balance, which is interfaced with a computer. The weight data is collected

and stored using data acquisition software. The lab balance lies upon a height adjustable platform that is set to the necessary height to provide the desired hydrostatic pressure at the eye.

The initial approach was to monitor the weight of the Petri dish in the incubator (see Appendix A). There are several advantages, however, to weighing the perfusate reservoir outside of the incubator. First, there is no size constraint for the weighing equipment, also which won't have to be subjected to the harsh environment (temperature and humidity) of the incubator. There is minimal weight interference from tubing, which hangs into the perfusate from a bracket on the draft shield of the balance. Using a custom height adjustable platform provides an opportunity to provide a mechanically stable environment for the balance.

There are also several considerations concerning the system design. One balance and one reservoir are required for each infused eye. A weight change resolution of 0.1 mg/min is necessary to meet the requirements set out above (the perfusate density is similar to water). Contact between the tubing and reservoir introduces errors in the weight measurements (therefore, there can be no reservoir cover). An open reservoir means that consideration must be given to possible perfusate contamination by airborne particles, and to perfusate evaporation, which could skew the weight change over time. The reservoir must be accessible to refill the perfusate levels or add pharmaceutical agents.

The system outlined above was first validated by a series of tests, and then implemented using porcine eye specimens. The design and methods are explained in detail.

CHAPTER 2

MATERIALS & METHODS

2.1 System Design

The system is describe in a modular method; beginning with the height adjustable platform. The instrumentation portion is then described, followed by the perfusion portion of the system.

2.1.1 Balance Platform

The platform design provides a mechanically stable environment for the balance, and a vertically adjustable surface. It consists of an aluminum bench (10”x 40”x 1”) and three threaded steel round stock legs (16” x 0.75” diameter); using three legs eliminates the possibility of wobbling. The legs are fastened to the bench at the desired length using nuts and washers (See Figure 2.1).

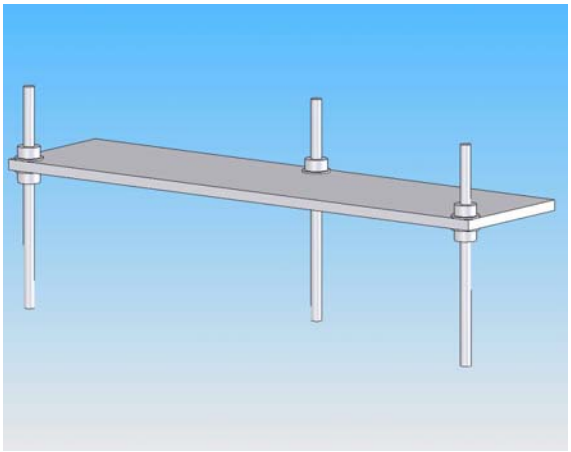

Figure 2.1: Height Adjustable Platform.

The aluminum bench is scaled to hold four balances. Its solid design is intended to filter out any vibrations or impact loads that may disturb the scales. ANSYS FEM analyses were conducted to quantify deformation of the platform and susceptibility to vibrations. Figure 2.2 shows a structural analysis of the platform with a uniform load of 60 pounds applied over the top surface to simulate the weight of the bench and scales. The bottom areas of the legs are constrained in all directions. Max stresses of 288 psi occur in the steel legs, and are well below the yield strength of steel (~ 50 E3 psi [8]), giving a safety factor of about 170. A maximum displacement of 8.5 E-4 inches occurs in the aluminum bench and is greatly exaggerated in figure 2.2.

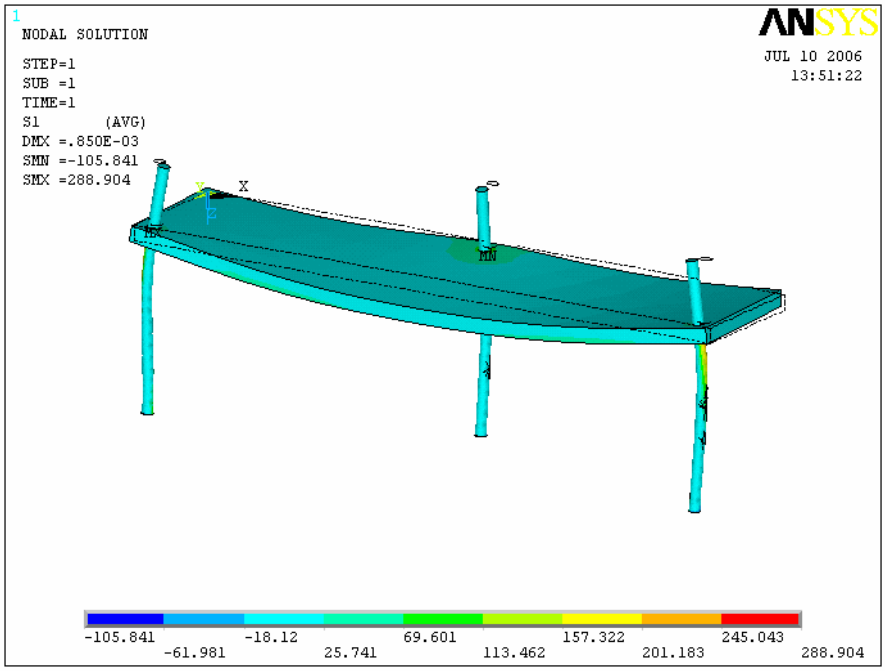

Figure 2.2: Structural Analysis of Platform

Modal analyses were also carried out to demonstrate the platforms resistance to high frequency vibrations. The leg lengths were set to a nominal value of 12”; shortening the legs would stabilize the platform. The first four modes were analyzed.

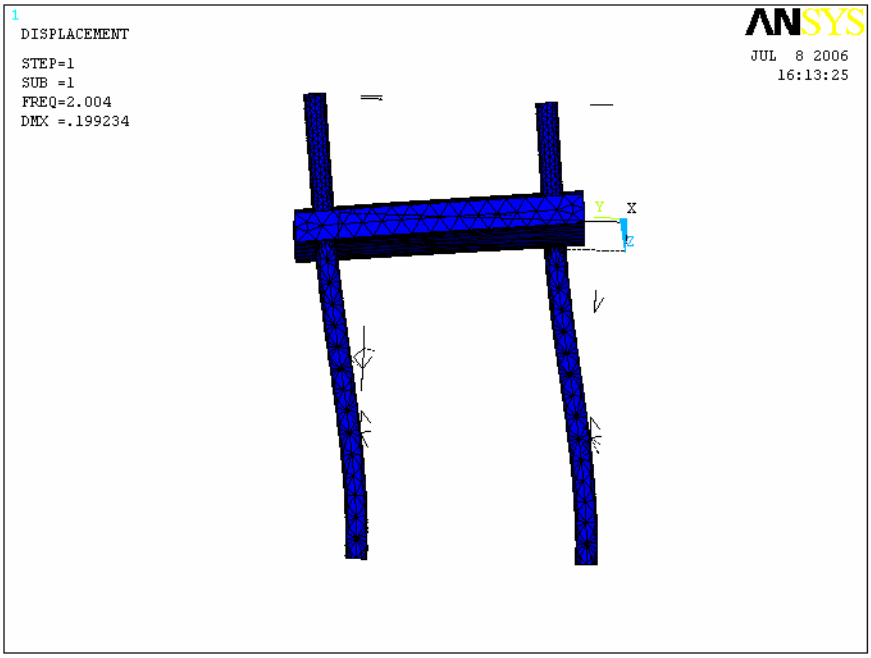

Figure 2.3: First Mode of Vibration

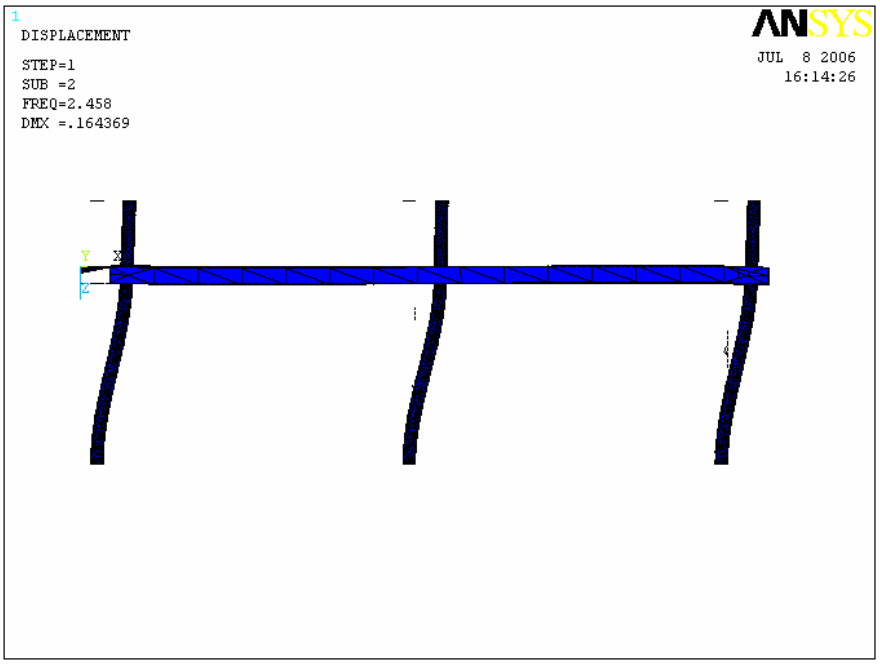

Figure 2.4: Second Mode of Vibration

Figures 2.3 and 2.4 show side views of the platform under the first two modes of vibration. They are side-to-side pendulum motions, and have natural frequencies of 2.004 Hz and 2.458 Hz, respectively.

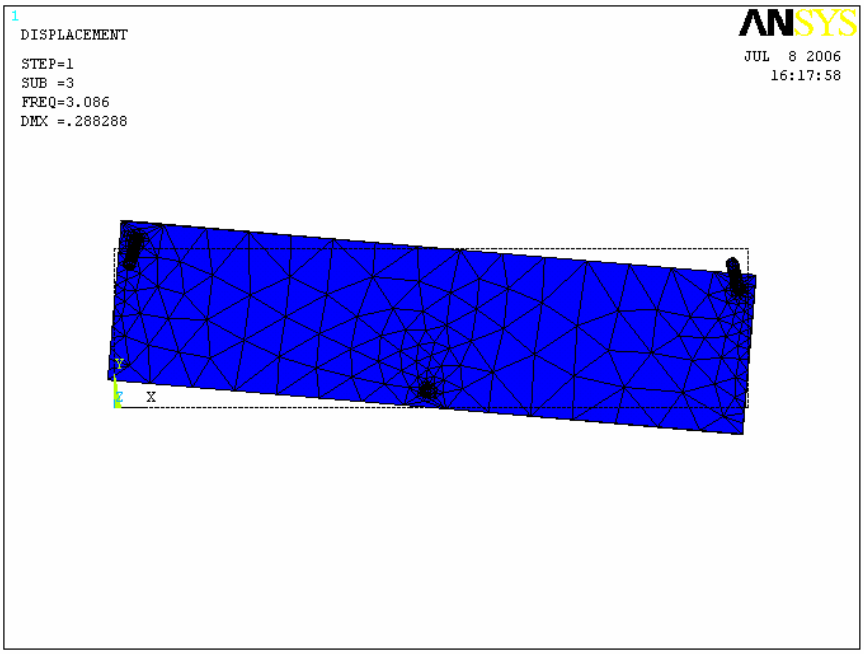

Figure 2.5: Third Mode of Vibration.

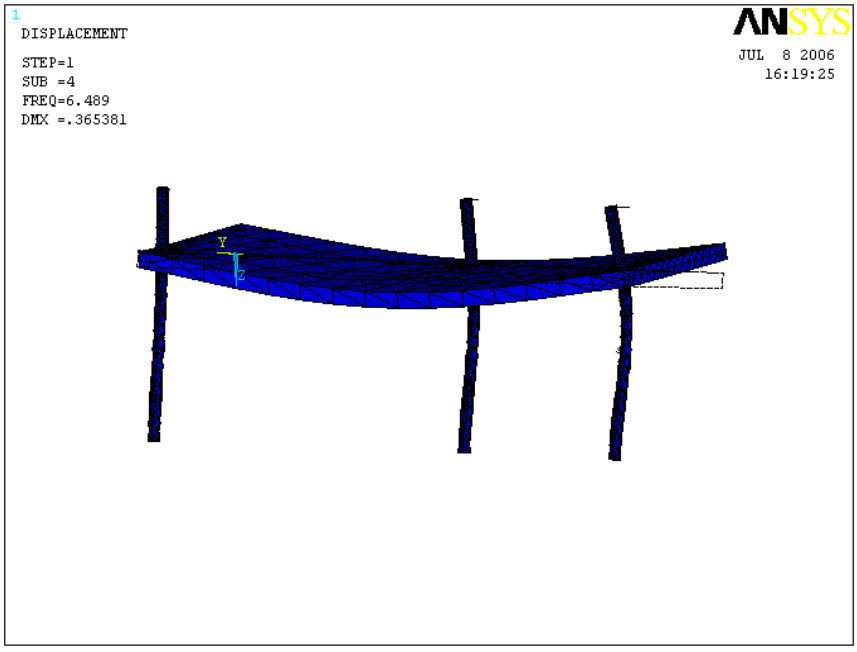

Figure 2.6: Fourth Mode of Vibration.

Figure 2.5 shows a top view of the third mode of vibration, a twisting motion of the platform, with a natural frequency of 3.086 Hz. Figure 2.6 shows the fourth mode of vibration; a bending motion of the bench, with a natural frequency of 6.489 Hz.

The modal analysis information is summarized in figure 2.7. The natural frequencies for the major modes of vibrations indicate the platforms stability. This conclusion is drawn due to stability of the environment; the strongest frequencies will be from footsteps, which aren't likely to match the natural frequencies found for the platform. The weight of the platform (45 lbs) filters out any impact loading.

Mode	Figure	Natural Frequency (Hz)	Type of Motion
1	2.3	2.004	Lateral Sway
2	2.4	2.458	Lateral Sway
3	2.5	3.086	Twisting Motion
4	2.6	6.489	Platform Bending

Figure 2.7: Summary of Vibration Modes.

2.1.2 Balance, Computer Interface, and Software

An ALC 110.4 lab balance from Acculab (Edgewood, NY 11717) is utilized in the system (see Appendix A for spec sheet). It has a range of 110 grams, a readability/repeatability of 0.1 mg, and a nonlinearity value of 0.3 mg. The readability was chosen to match the desired weight change resolution. The balance's 25 pin RS-232 port is interfaced with a computer USB 2.0 port via an Acculab LAT-CAB 25 pin RS-232 to 9 pin RS-232 converter cable and an IOGEAR 9 pin to USB 2.0 cable. The

interface allows for data acquisition software (WinWedge Std) to communicate with the balance and record weight values to a database on a regular interval, chosen by the user.

Figure 2.8: Core Components of System.

Figure 2.8 shows the basic components of the system, including the scale, reservoir, Petri dish, and computer/interface. It does not include the incubator, platform, perfusate, or an eye specimen.

2.1.3 Reservoir and Tubing

A 50 mL Erlenmeyer flask is used as the reservoir. It weighs about 40 grams, leaving enough range on the balance for the perfusate. The perfusate is protected from

possible contamination by the balance's draft shield and the provided dust cover. These two levels of protection supplement antibiotics [5] in the perfusate.

The tubing is supported by a bracket on a custom top door on the draft shield (see figure 2.9); the tubing hangs into, and only contacts the perfusate.

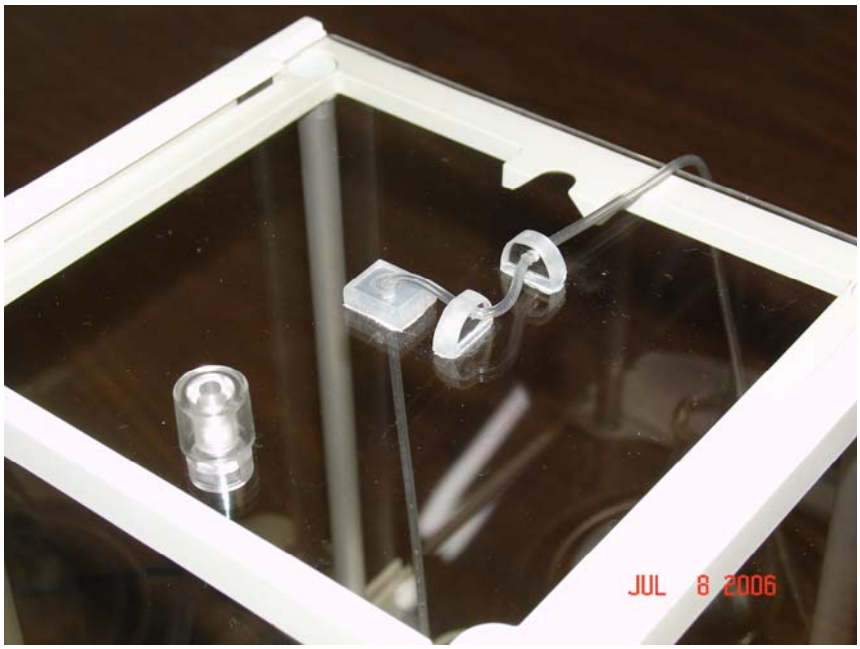

Figure 2.9: Custom Draft Shield Top with Tube Bracket.

The bracket mechanically isolates the portion of tubing inside the draft shield, protecting the perfusate from any mechanical disturbances transmitted along the tubing.

Fluid flow is so small (Velocity ≈ 0.55 cm/min, Reynolds number ≈ 0.06; see Appendix C) that hydrodynamic resistance of the tubing is negligible and the perfusate has ample time to warm up in the incubator before it reaches the eye specimen.

2.2 System Validation

A set of experiments was designed to validate the stability, tracking capabilities, and resolution of the system. The experiments were run long enough to obtain a trend line. Once acceptable validation data was obtained, the system was set up with a porcine eyeball specimen to demonstrate its effectiveness in measuring fluid flow.

Figure 2.10: Set up for Porcine Eye Perfusion Tests.

Figure 2.10 shows the setup for the porcine eye perfusion test; a makeshift platform was utilized for these tests. The incubator can be seen on the left; pressure sensors are on the door of the incubator.

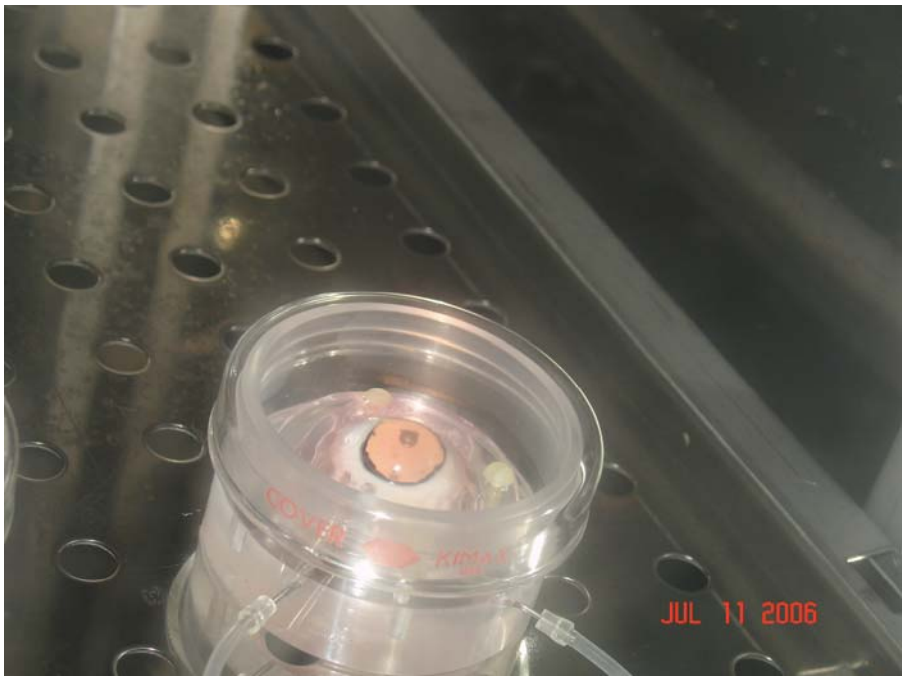

Figure 2.11: Porcine Eye in Incubator during Perfusion.

Figure 2.11 shows a porcine eye specimen under perfusion. The perfusate can be seen around the eye after it has flown through the AH outflow network.

2.2.1. Balance's Static Stability

The purpose of this experiment was to determine the long term static stability of the balance, and the maximum rate of change in the balance output, under constant loading. Output changes above this maximum rate of change can be attributed to true weight changes. A weight (a 50 mL Erlenmeyer flask) was placed on the balance and left for 4 days; weight data was recorded every 5 minutes over this time.

2.2.2. Quantifying Evaporation

The reservoir was filled with water and left on the scale for a period of time to determine the balance's ability to track the weight change due to evaporation, and to quantify the evaporative rate. The evaporative rate is used as a control for the flow rate, since stable environmental conditions (temperature, pressure, and humidity) are maintained. Evaporation was quantified as being minute and predictable, due to the stable environment.

2.2.3 Balance's Dynamic Capabilities

The evaporation tests demonstrated the balance's ability to stably track weight changes, but further attention was given to the balance's dynamic capabilities. Two flow tests were conducted to test these capabilities.

The first test was to connect a pipette to the tubing, and add and remove 10, 5 and 3 μL of fluid to and from the reservoir. The purpose of this test was to further validate the balance's ability to monitor weight changes due to μL scale fluid changes.

The second test was to place the tube outflow at a level below the fluid level and allow the fluid to siphon out. The purpose of this test was to demonstrate the long term flow monitoring ability of the system. Theoretical flow rates for the initial water level and final water level were compared to flow rates measured by the system.

2.2.4 Effects of Fluid Level Changes

The change in fluid level due to outflow from the reservoir (including evaporation) affects the hydrostatic pressure and the buoyancy effects of the tubing. Assuming a nominal flow of 2.5 μL/min through the AH outflow network, there will be an outflow of 3.6 mL/day from the reservoir. This outflow will change the perfusate level in the reservoir by about two millimeters, assuming the reservoir is filled to the 30 mL mark. The intended users of the system have deemed this minute fluid level change, over such a long period of time, as negligible where pressure and tube buoyancy effects are concerned.

2.3 Data Processing

Collected data must be manipulated to obtain a flow rate with an acceptable resolution. Equation 2.1 expresses the flow rate obtained from the weight data, taking evaporation into consideration.

$$Q = (\Delta W/\Delta t - E)/\rho \qquad \text{Eq. 2.1}$$

Where:

Q – flow rate (mL/min).
$\Delta W/\Delta t$ – is the weight change over time as recorded by the balance (g/min).
E – evaporative rate (g/min); empirically found and assumed to be constant
ρ – density of the perfusate (g/mL); a density value of 1g/mL is used.

A low sampling rate, high Δt, improves the confidence of the $\Delta W/\Delta t$ value over the time span (discussed later), but decreases the time resolution; only the average rate of change over Δt is known for each Δt period. A method to determine a range of error is described later.

CHAPTER 3

RESULTS

3.1 Static Stability Data

Results from static stability tests are shown below; figure 3.1 shows the weight vs. time of a 50 mL Erlenmeyer flask recorded by the balance over 4 days. Data was collected every 5 minutes.

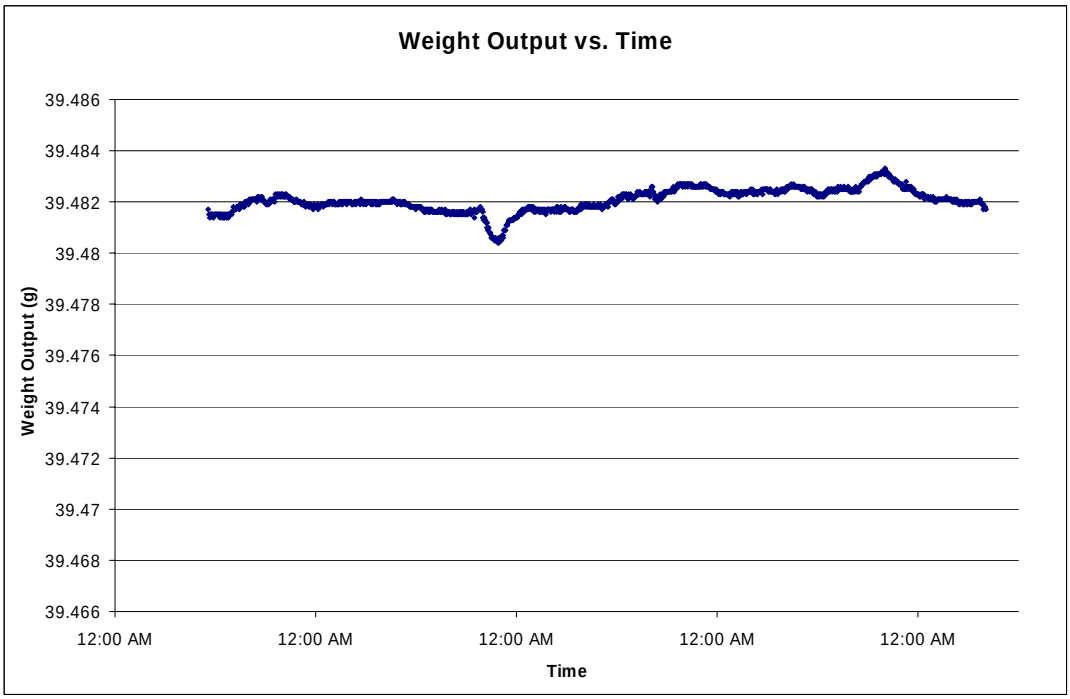

Figure 3.1: Weight vs. Time of Erlenmeyer Flask.

The observed fluctuation in the output is attributed to the nonlinearity (0.3 mg) of the balance.

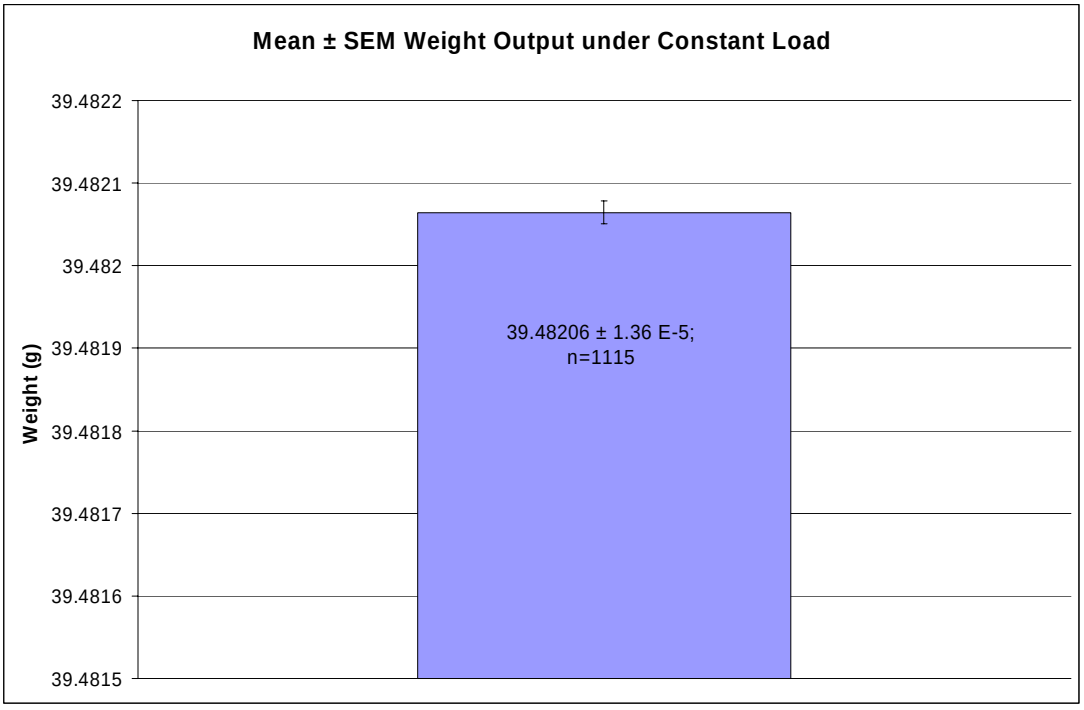

Figure 3.2: Mean ± SEM of Weight Output under Constant Load

Figure 3.2 shows data from figure 3.1 as 39.482065 ± 1.36 E-5 g (mean ± SEM; n=1115). The low standard error value validates the static stability of the balance. Since we are interested in the balance's ability to track changes in weight over time, weight data from figure 3.1 was differentiated to give figure 3.3.

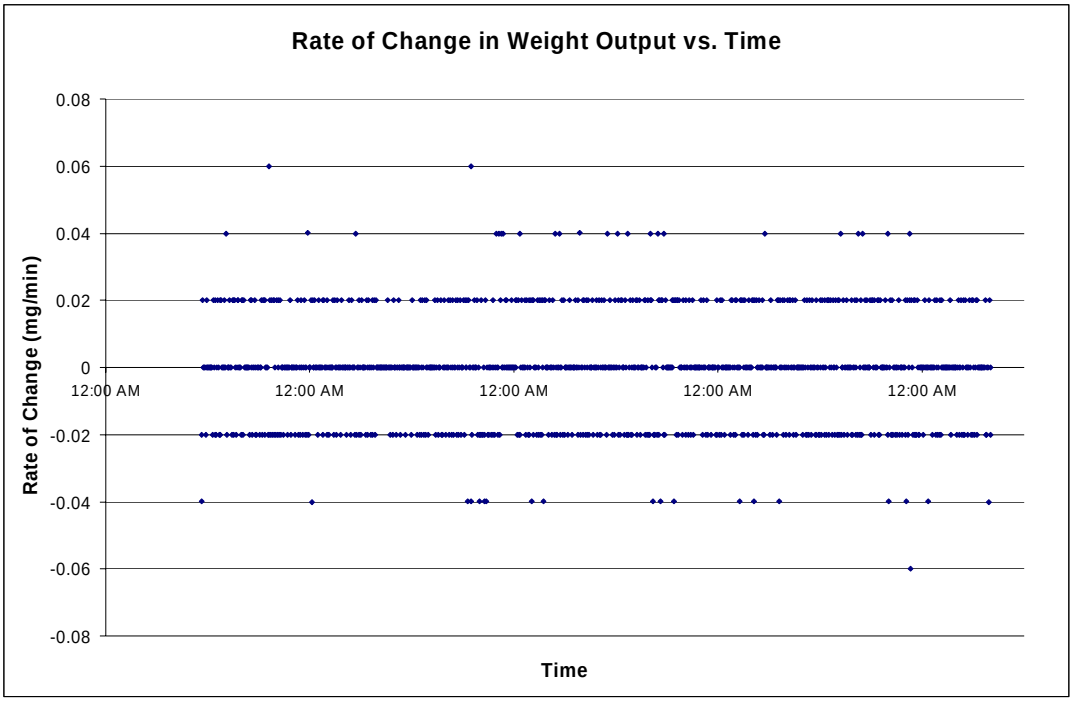

Figure 3.3: Rate of Change in Weight Output vs. Time

Figure 3.3 shows the change in weight output (mg/min) over time, under constant loading, which ideally should be zero; the average of which is -6.08 E-24 (virtually zero) ± 3.15 E-5 g/min (mean ± 2 SD). Two standard deviations were used to determine a 95 % confidence level ($\alpha = 0.05$) in weight changes recorded by the balance.

3.2 Evaporation Data

The reservoir was filled with water and placed on the balance to demonstrate its ability to quantify evaporative rates; two water tests were conducted. Data was acquired every minute.

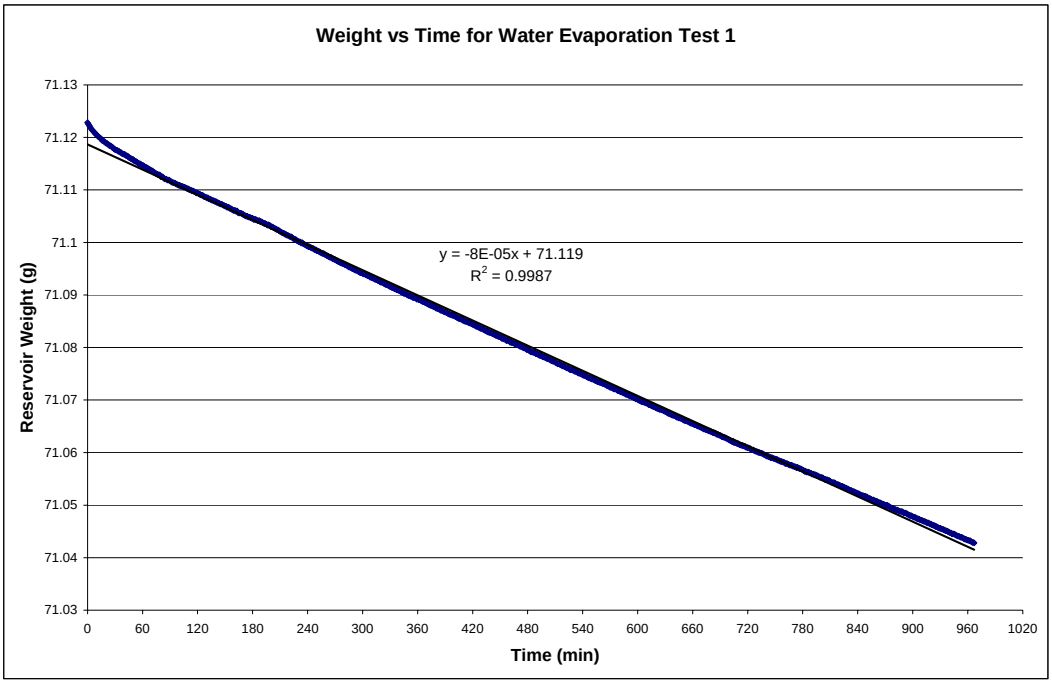

Figure 3.4: Reservoir Weight vs. Time for Water Evaporation Test 1.

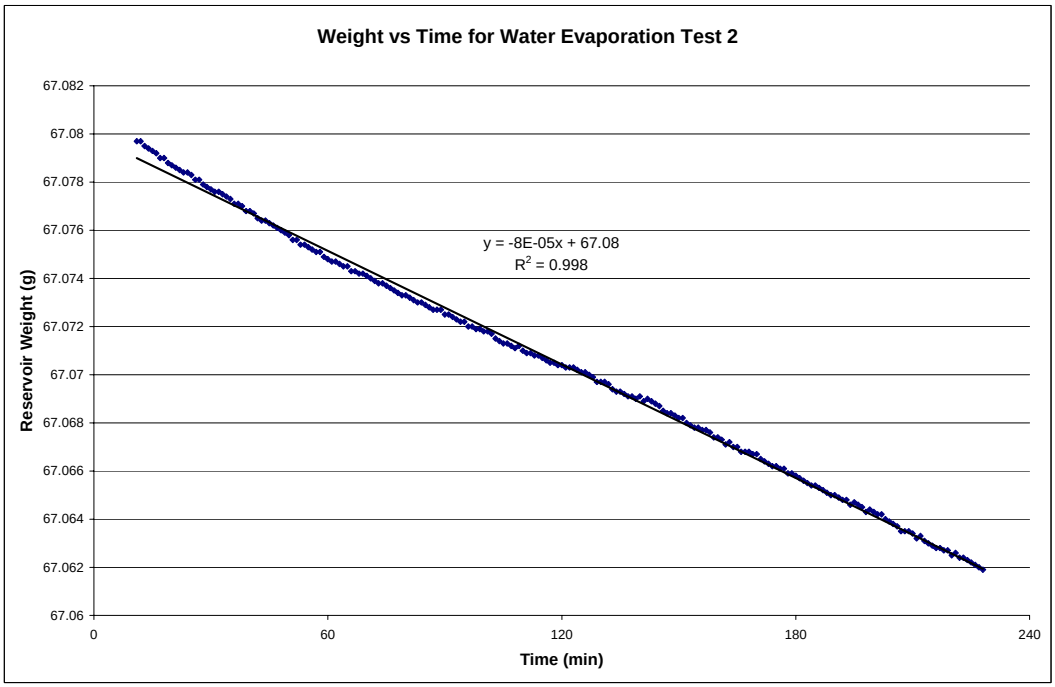

Figure 3.5: Reservoir Weight vs. Time for Water Evaporation Test 2.

Figures 3.4 and 3.5 show the reservoir weight over time as water is evaporating; both tests display a nice trend line, with R^2 values of 0.9987 and 0.998 respectively.

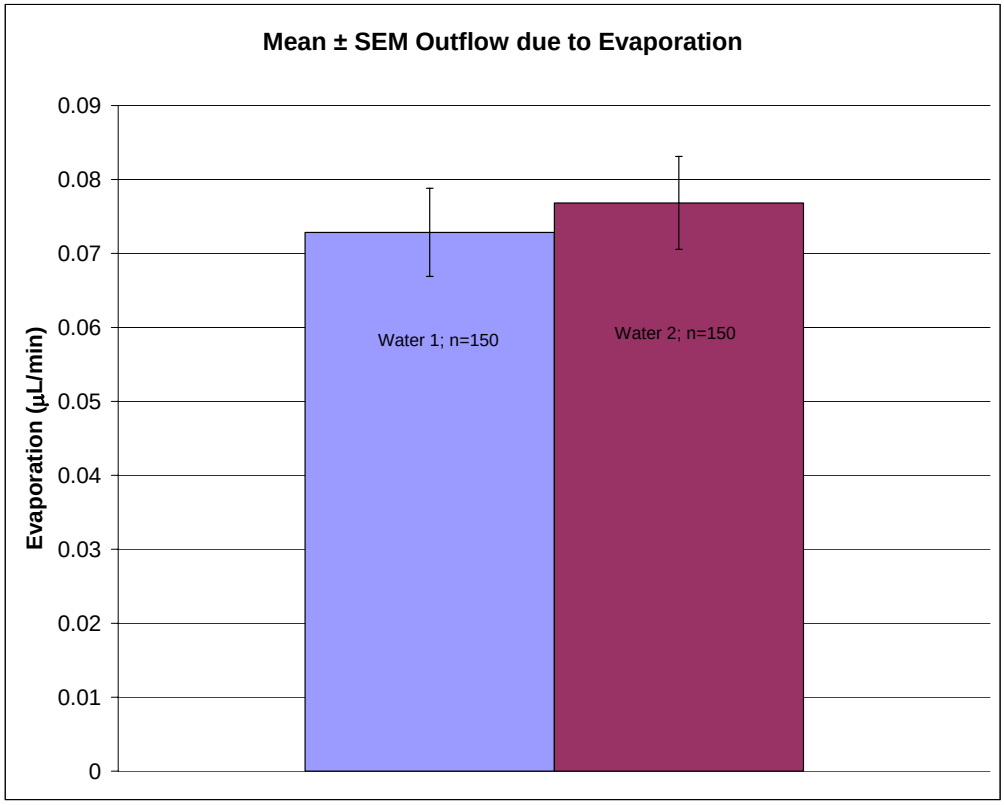

Figure 3.6: Mean ± SEM Evaporative Rates.

Figure 3.6 shows the evaporative rates as 0.0728 ± 0.0060 µL/min and 0.0768 ± 0.0063 µL/min (means ± SEM; n = 150) for water tests 1 and 2 respectively. These values were obtained by differentiating, converting mg to µL, and averaging the data from figures 3.4 and 3.5. The evaporative rates were averaged, since they are theoretically constant, due to the stable environment described above.

3.3 Flow Data

3.3.1 Pipette Flow Data

A pipette was connected to the end of the tube where the Petri dish would normally be; 10, 5, and 3 μL of water were introduced to and removed from the reservoir to simulate perfusate flow (see figure 3.7). Data was collected every 3 seconds.

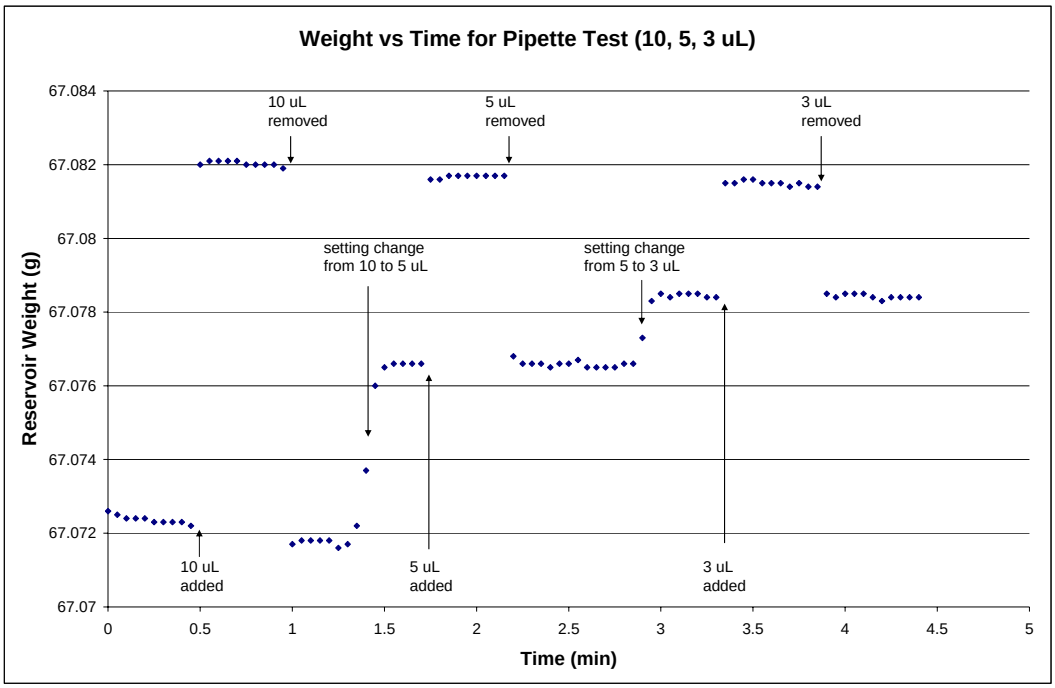

Figure 3.7: Reservoir Weight vs. Time for Pipette Test (10, 5, 3 μL).

The weight discontinuities in figure 3.7 indicate the addition and removal of fluid using the pipette. The weight changes at 1.4 and 2.9 minutes indicate the pipette setting being changed from 10 to 5 μL and 5 to 3 μL respectively. The slight downward drift is due to evaporation. As can be seen, the balance did very well in tracking the

weight changes. Figure 3.8 was obtained differentiating data in figure 3.8 over each time interval.

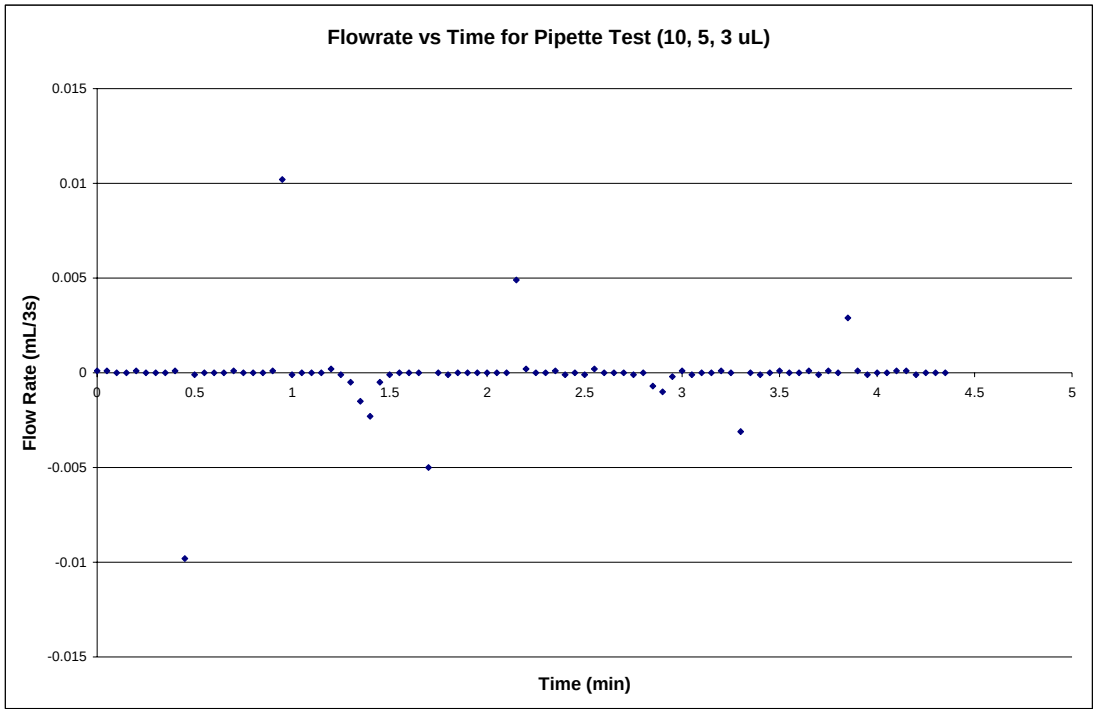

Figure 3.8: Flow Rate vs. Time for Pipette Test (10, 5, 3 μL).

Figure 3.8 shows the flow rates corresponding to the fluid additions and losses shown in figure 3.7. Flow rate is expressed in mL/3s, 3 seconds being the sampling interval. The flow is negative for fluid is entering the reservoir. The fluid flows show up as a single data point; the pipette adjustments mentioned above show up as the two negative deviations at 1.4 and 2.9 minutes.

3.3.2 Free Flow Data

The reservoir was filled and the outflow end of the tube was placed at a level below the water level. Water was allowed to siphon out; data was collected every minute.

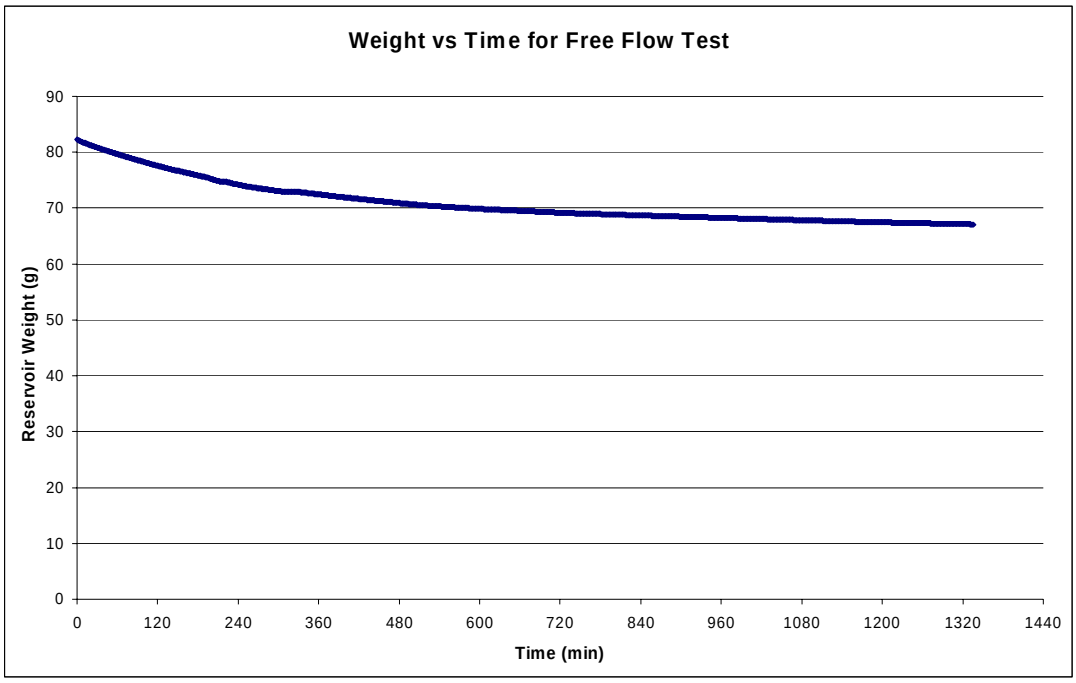

Figure 3.9: Reservoir Weight vs. Time for Free Flow Test.

Figure 3.9 shows the weight of the reservoir over time for the free flow test. The corresponding flow rates are obtained by differentiating the data in figure 3.9 over each sampling time interval (see figure 3.10).

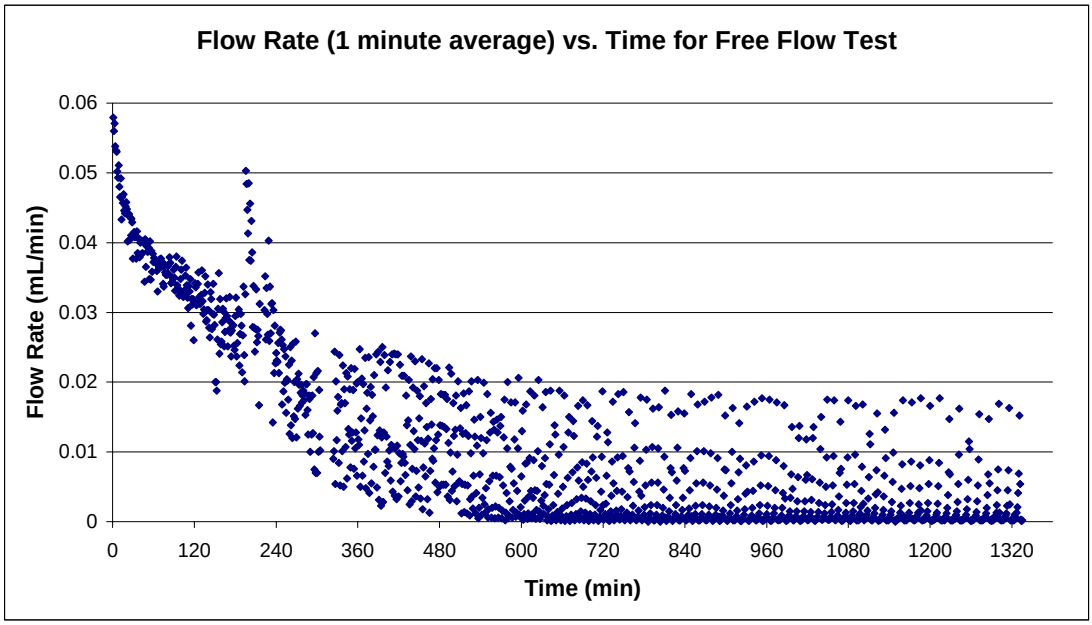

Figure 3.10: Flow Rate (1 minute average) vs. Time for Free Flow Test.

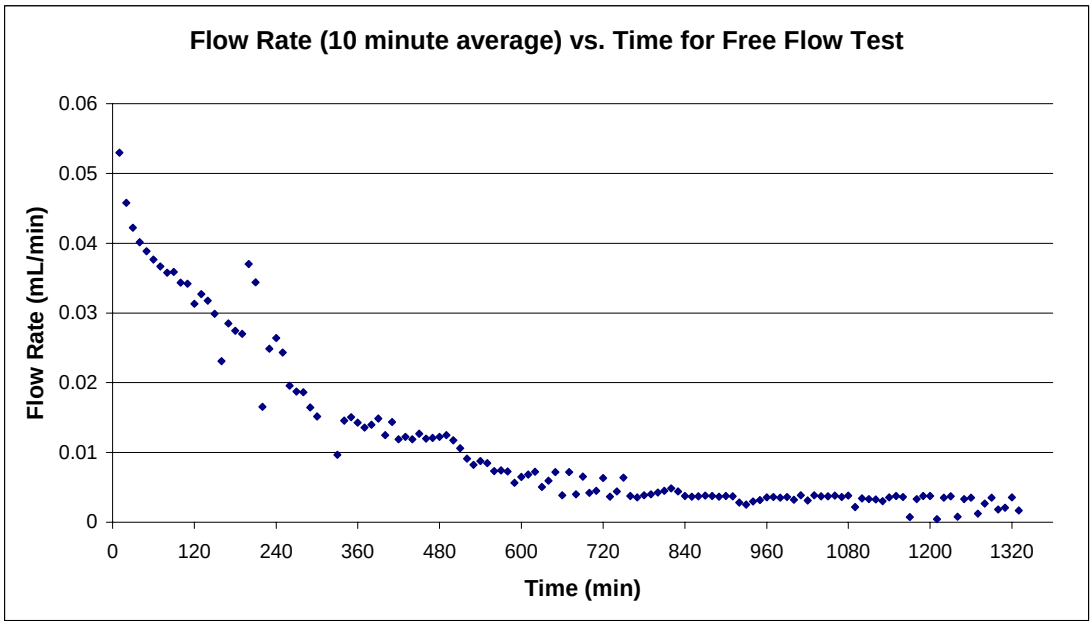

Figure 3.11: Flow Rate (10 minute average) vs. Time for Free Flow Test.

The disturbance at 200 minutes was due to contact between the tube and the reservoir; when this problem was fixed, the data resumed its previous trend. The flow rate data in figure 3.10 appears to be quite chaotic; zooming in, however, shows that it is very orderly (see figures 3.12 and 3.13). The data also becomes more orderly when the flow rates are averaged over 10 minute intervals (see figure 3.11).

There was a 1.3 cm change in fluid level during the test run (Δz_1 = 1.9 cm; Δz_2 = 0.6 cm). Theoretical flow rates for these Δz values are 0.1 and 0.03 mL/min respectively (see Appendix C). Due to the effects of the surface tension (described below), the measured flow rates are smaller than these theoretical flow rates.

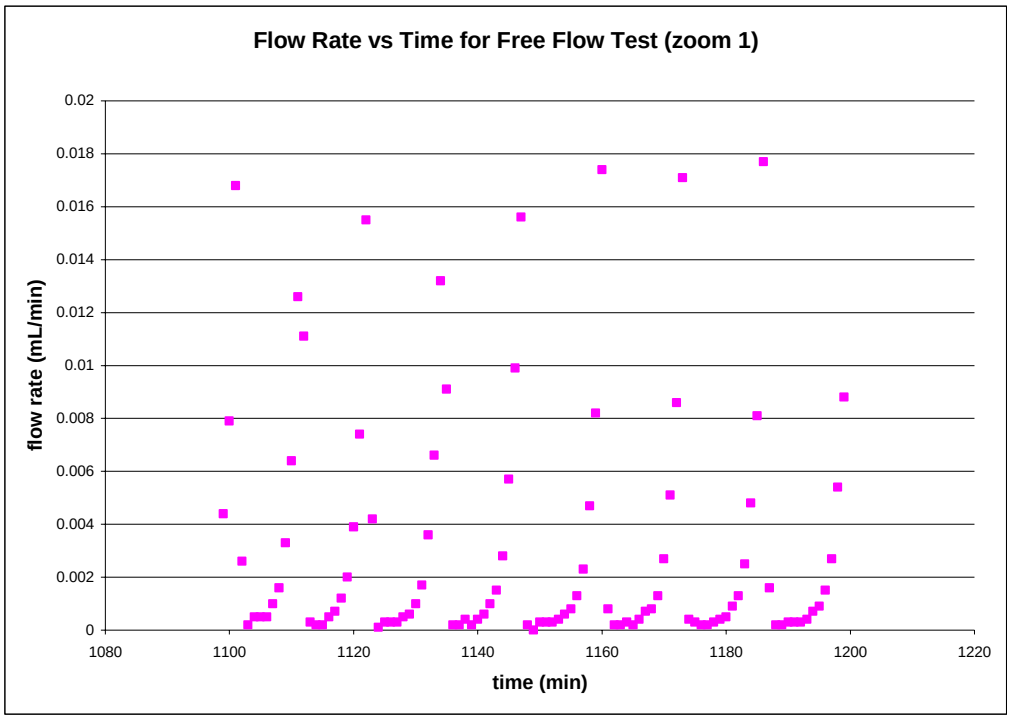

Figure 3.12: Flow Rate vs. Time for Free Flow Test (zoom1).

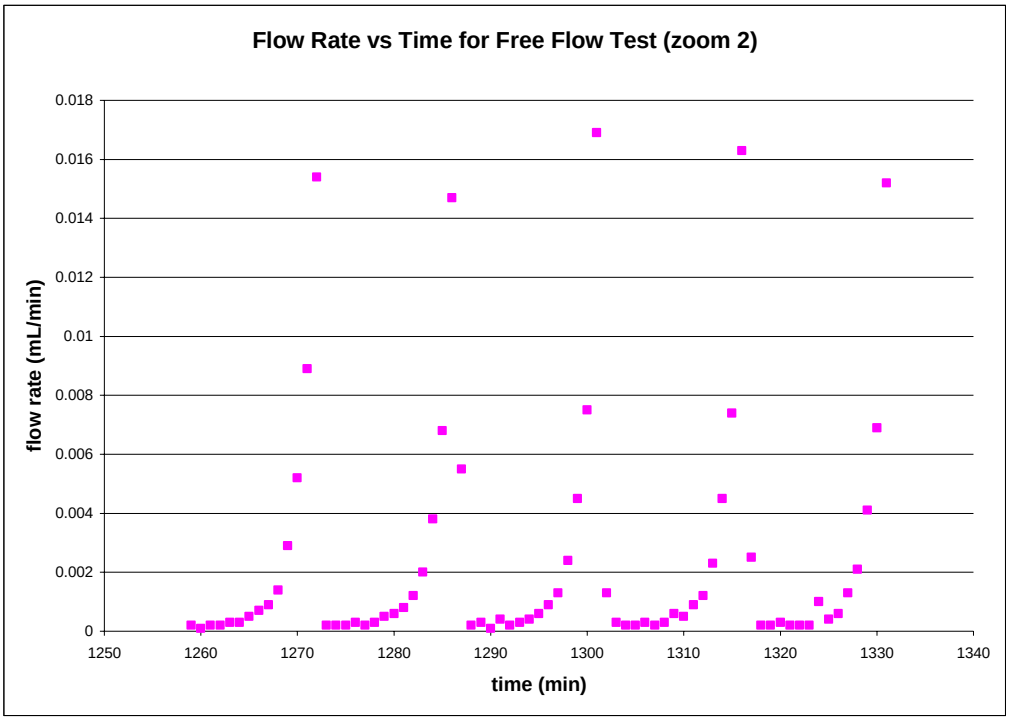

Figure 3.13: Flow Rate vs. Time for Free Flow Test (zoom2).

The variable flow rates in figures 3.12 and 3.13 can be attributed to the water dripping out the end of the tube (see figure 3.14). As a drip builds up, the flow increases due to the lowered surface tension at the tube output and the pulling effect of the water droplet. When the drop drips, the flow decreases drastically, as the tube pressure must overcome the surface tension of the water in order to push out a new drop. This effect is responsible for lowering the flow rate from the theoretical flow rate, as mentioned above. The time between drips increased from roughly 5 to 12 minutes from the 1140th minute to the 1290th minute (see Figures 3.12 and 3.13); due to the decreased hydrostatic pressure.

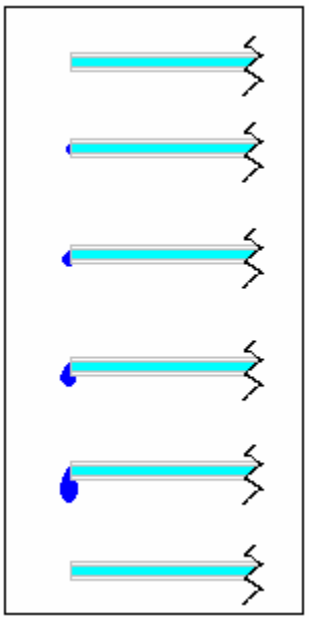

Figure 3.14: Progression of Drop Forming on End of Tube

Figure 3.14 illustrates the progression of a drop forming and dripping. This phenomenon will not occur during the intended use of the system, as there will be no opportunity to develop surface tension.

3.4 Porcine Eye Perfusion Data

3.4.1 Porcine Eye Perfusion Test with Corneal Puncture

The system was set up with a porcine eye and allowed to run for about 17 hours; an evaporative calibration test was first conducted. The cornea was punctured at minute 941 with a 27 gauge needle to check if the system could track the corresponding flow rate increase. Data was collected every minute.

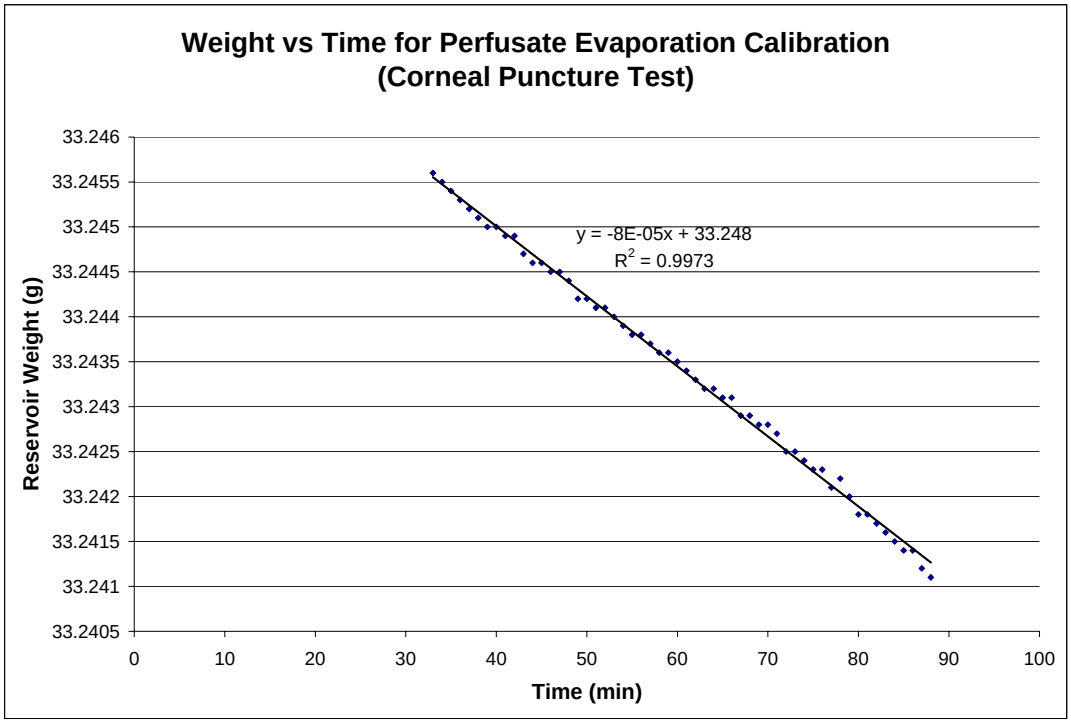

Figure 3.15: Reservoir Weight vs. Time for Evaporation Calibration (Corneal Puncture Test)

Figure 3.15 shows the reservoir weight vs. time for the perfusate evaporation calibration test. The evaporative rate was determined to be 0.0818 ± 0.00948 μL/min (mean ± SEM; n=54) from data in figure 3.15, and used to adjust the flow rates obtained in the porcine eye perfusion corneal puncture test.

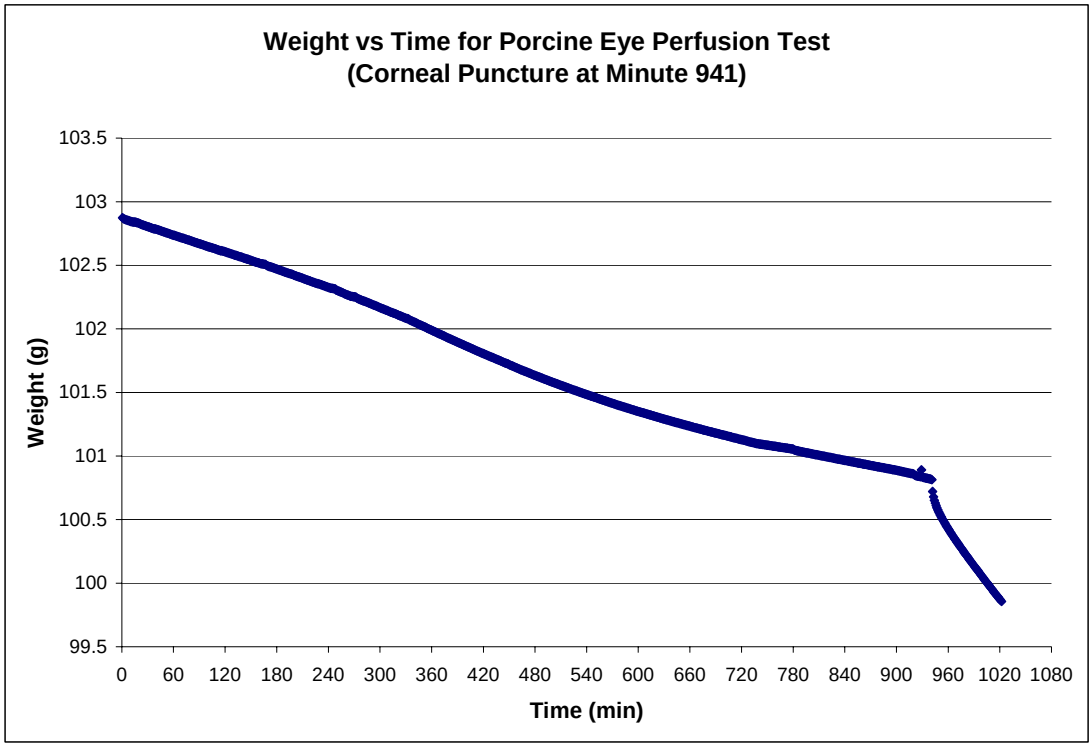

Figure 3.16: Reservoir Weight vs. Time for Porcine Eye Perfusion Test (Corneal Puncture at Minute 941).

Figure 3.16 shows the weight of the perfusate reservoir during the porcine eye perfusion test. The slope change at minute 941 corresponds to the corneal puncture. The weight data was differentiated over one and ten minute intervals to obtain flow rates, which were adjusted for evaporation (see figures 3.17 and 3.18 respectively).

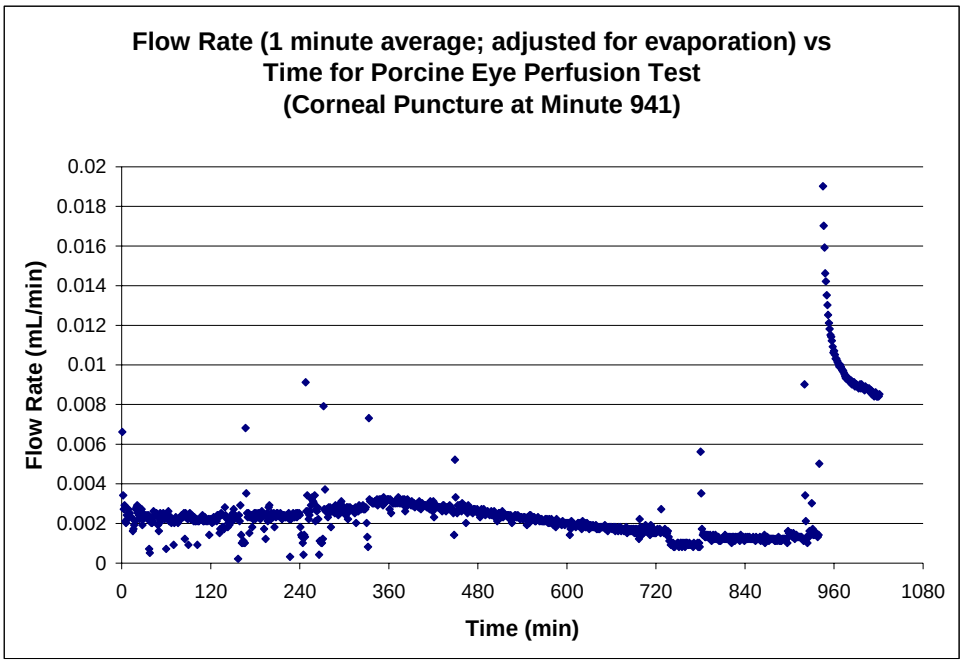

Figure 3.17: Perfusate Flow Rate (1 minute average; adjusted for evaporation) vs. Time for Porcine Eye Perfusion Test (corneal puncture at minute 941).

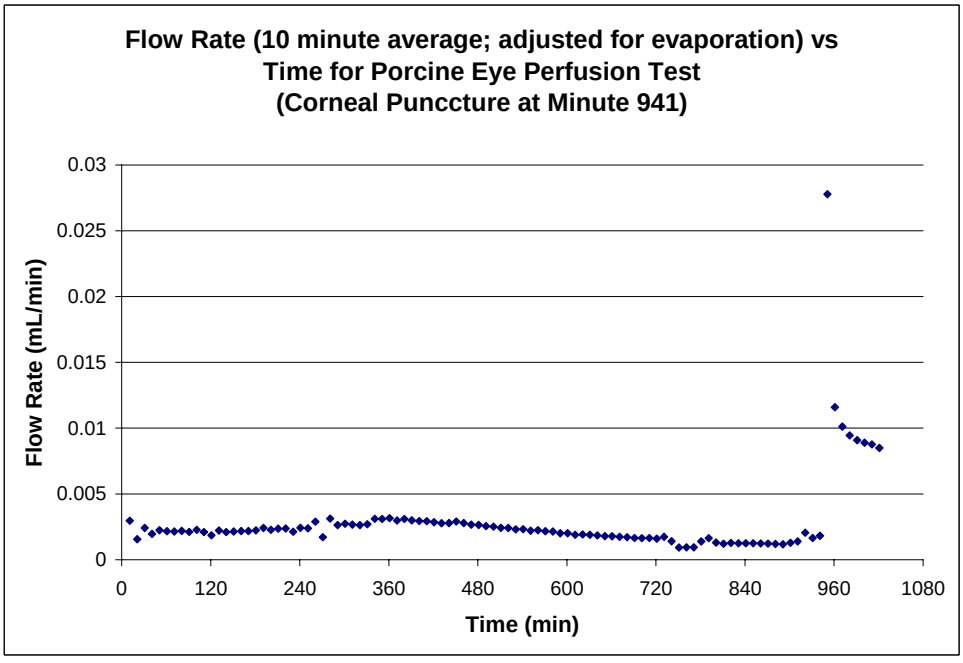

Figure 3.18: Perfusate Flow Rate (10 minute average; adjusted for evaporation) vs. Time for Porcine Eye Perfusion Test (corneal puncture at minute 941).

Figures 3.17 and 3.18 show the flow rate data (adjusted for evaporation) for the porcine eye perfusion test, with a corneal puncture at minute 941. Averaging the data over ten minutes creates less noise, but both figures demonstrate the increase in flow rate due to the corneal puncture.

3.4.2 Porcine Eye Perfusion Test with added Pharmaceutical Agent

A second pig eye perfusion test was conducted to demonstrate the effect of adding a pharmaceutical agent (compound X; provided by Dr. Pang of Alcon Laboratories) to the perfusate; the compound is a trade secret. An evaporative calibration test was first conducted.

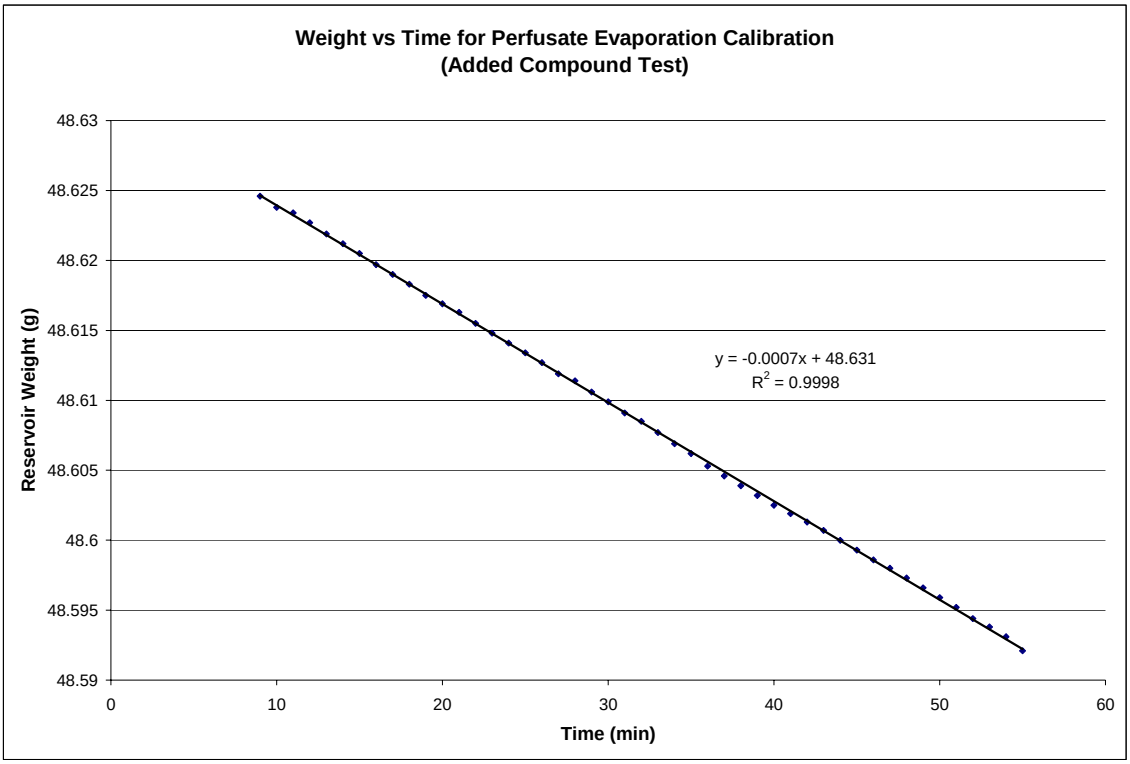

Figure 3.19: Reservoir Weight vs. Time for Evaporation Calibration (Added Compound Test).

The evaporative rate was determined to be 0.709 ± 0.0147 μL/min (mean ± SEM; n=46) from data in figure 3.19; the evaporative rate is higher for this test because a different reservoir was used. This evaporative rate is used to adjust the flow rates obtained in the porcine eye perfusion drug test.

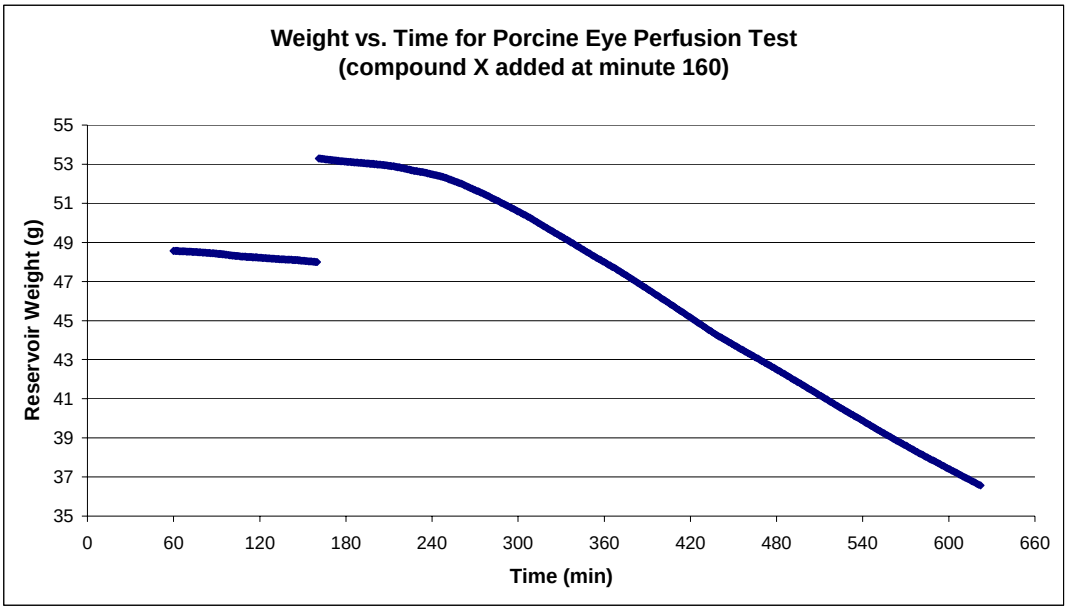

Figure 3.20: Reservoir Weight vs. Time for Porcine Eye Perfusion Test (compound X added at minute 160).

Figure 3.20 shows the reservoir weight vs. time during the porcine eye perfusion test. The weight discontinuity at minute 160 is due to the addition of compound X. One and ten minute flow rate averages were obtained by differentiating and averaging data from figure 3.20 (see figures 3.21 and 3.22 respectively); flow rates were adjusted for evaporation.

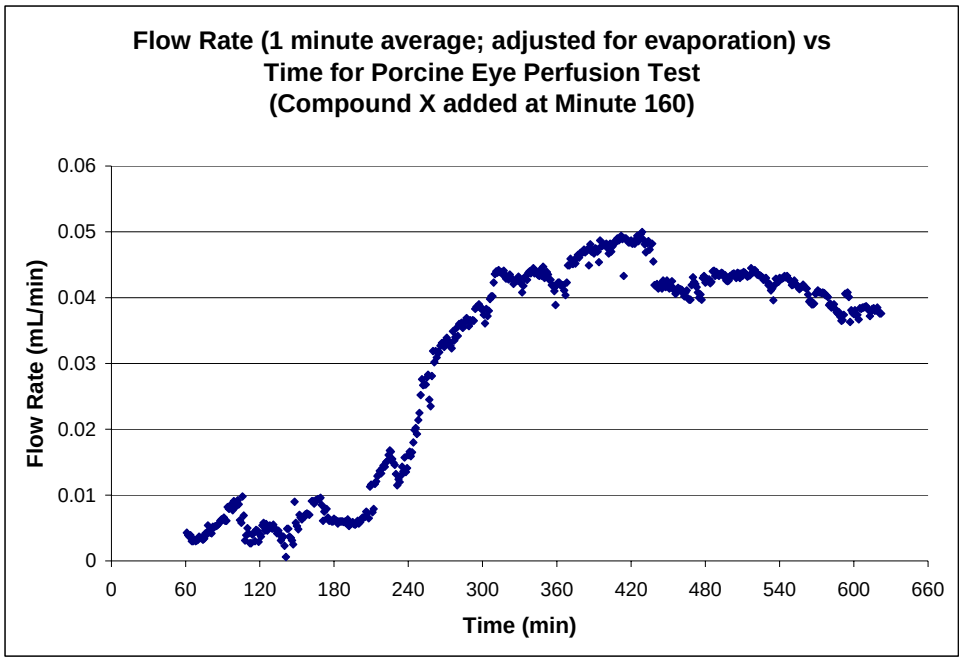

Figure 3.21: Perfusate Flow Rate (1 minute average; adjusted for evaporation) vs. Time for Porcine Eye Perfusion Test (compound X added at minute 160).

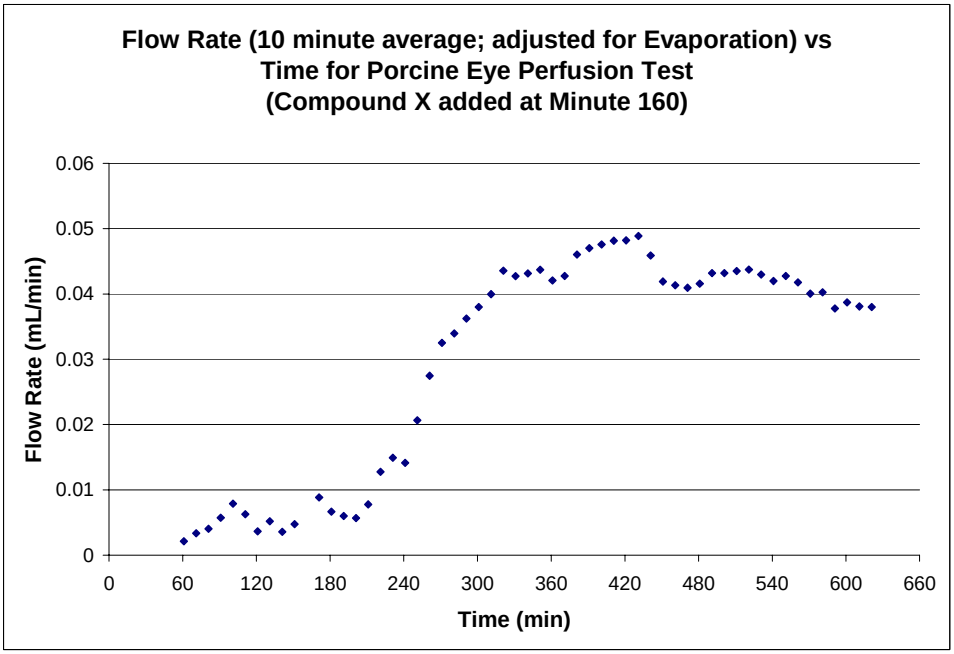

Figure 3.22: Perfusate Flow Rate (10 minute average; adjusted for evaporation) vs. Time for Porcine Eye Perfusion Test (compound X added at minute 160)

Figures 3.21 and 3.22 both demonstrate an increase in perfusate flow rate due to the addition of compound X; again, averaging the flow rate over ten minutes clears up the noise in the data. The standing theory is that toxicity of compound X causes an increase in flow through the AH outflow network.

CHAPTER 4

DISCUSSION

4.1 Method

A system and method were developed to measure the flow rate of perfusate through the aqueous humor outflow network of a human eye under constant pressure. The system includes a lab balance, height adjustable platform, and a computer with data acquisition software. The following is a method summary for the system.

The platform level is set to provide the desired hydrostatic pressure at the eye. The perfusate reservoir is filled with perfusate and placed on the balance; the tubing is placed in the bracket on the custom top door of the draft shield, and a straightened section is allowed to hang into the perfusate. The tubing is connected to the modified Petri dish, which holds an eye specimen. The Petri dish is placed in the incubator and perfusate begins to flow through the aqueous humor outflow network. Perfusate reservoir weight data is collected on a regular interval over the entire test run, and later converted to a flow rate using equation 2.1.

The perfusate must be refilled to the original level on a regular interval in order to maintain the desired hydrostatic pressure; the interval depends on the flow rate, but once daily will suffice for nominal flow rates.

4.2 Control

It was found that higher quality data was obtained by permitting evaporation, and later compensating for it, instead of sealing the reservoir to prevent evaporation. To control for evaporation, a calibration run must be done to obtain the evaporative rate for the specific fluid, reservoir, and environmental conditions; this value is used to adjust the flow rates. Water can be added daily, to compensate for the small amount lost to evaporation, if specific perfusate concentrations need to be maintained.

4.3 Range and Resolution

The system is more than capable of measuring flow rates within the required range (0 – 10 μL/min); figure 3.20 demonstrates a measured flow rate of 50 μL/min. The main consideration for the range is the amount of fluid lost, which affects the time between refilling the perfusate level. Other important considerations are the flow rate and time resolutions of the system.

The nonlinearity of the balance (0.3 mg) is the highest source of error in the system. A range of uncertainty for flow rate values can be found using this value, by dividing it, along with ΔW from equation 2.1, by the Δt value. Therefore, a higher confidence can be obtained by increasing the Δt value from equation 2.1 (decreasing the time resolution). For example, a weight change recorded over 10 minutes will give an uncertainty range of ± 0.03 mg/min ($W_1 \pm 0.15$ mg - $W_2 \pm 0.15$ mg / 10 minutes = $\Delta W/\Delta t \pm 0.03$ mg/min); giving an inverse relationship between the time resolution and flow rate resolution. This relationship is expressed by $\pm X = 0.3\text{mg}/\Delta t$; where "± X" is

the range of uncertainty (mg/min), 0.3 mg is the nonlinearity value, and Δt is the time interval (min). This inverse relationship can be manipulated to obtain acceptable data confidence and time resolution. Again, mg and μL can be interchanged freely, since the fluids used are virtually water ($\rho = 1$ g/mL).

4.4 Conclusion

The purpose of this project was fulfilled, with a system capable of measuring flow rates on the μL/min scale, and methods to control for evaporation and determine time and flow rate resolutions.

The system can be applied to any situation requiring quantification of flow rates on the scale mentioned above, including the perfusion of alternate organs and tissues. Future work includes the expansion of the prototype to multiple units and corresponding software modifications.

APPENDIX A

INITIAL DESIGN

Initial Approach and Design

The initial approach was to weigh the Petri Dish in the incubator. An application specific scale was designed to hold the modified Petri dish and measure the weight in real time; it was built from 0.22" acrylic sheet. The weight amplifying and transferring (WAT) device consists of a triangular platform (figure A.1), which rests on the effort arms of three identical first-class levers (L1).

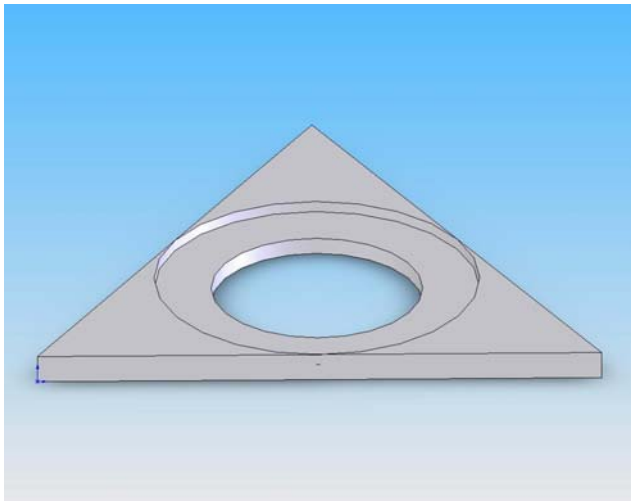

Figure A.1: Triangular Platform

The L1 levers are arranged radially at 120 degrees, with the resistance arms meeting centrally and contacting the effort arm of an inverted first-class lever (L2). The L2 lever's resistance arm contacts a load cell. Figure A.2 shows the base, levers, and fulcrums.

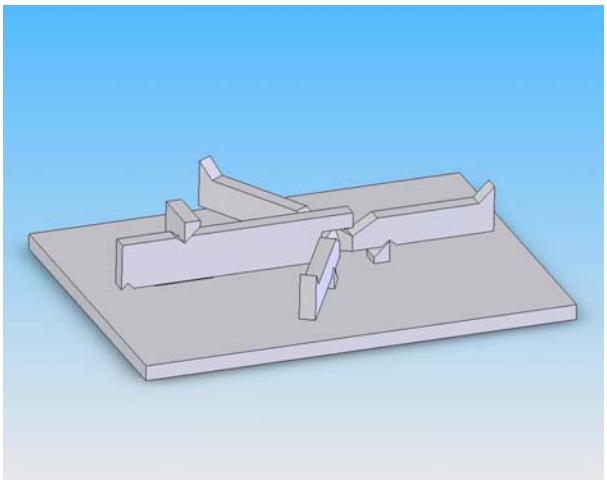

Figure A.2: Lever System of WAT Device

The platform and levers are oriented by guiding rails, which prevent motion other than rotation about the fulcrum for the levers and y-direction translation for the platform (base lies in y-plane). The dish tubing is held in place by brackets which allow it to be "snapped" in and out. The Petri dish is oriented by the circular cutout of the platform. Figure A.3 shows the base with guiding rails, tube brackets and fulcrums.

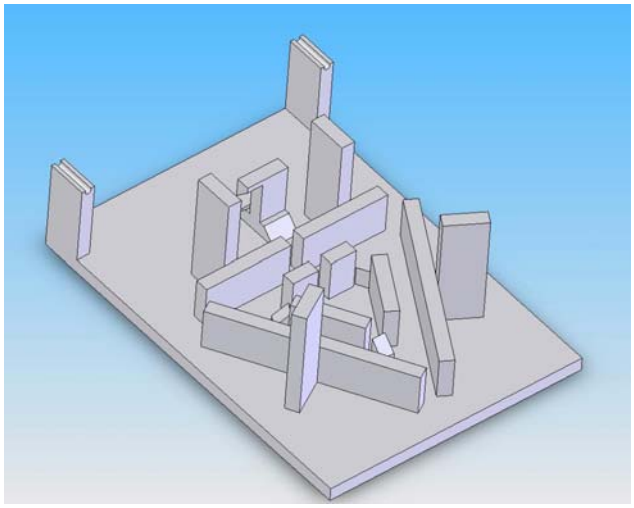

Figure A.3: Base with Guides, Fulcrums, & Tube Brackets

The tube brackets keep the tubing from interfering with the weight measurements, providing an invariable finite weight effect. Figure A.4 shows the total device (load cell and dish are not shown).

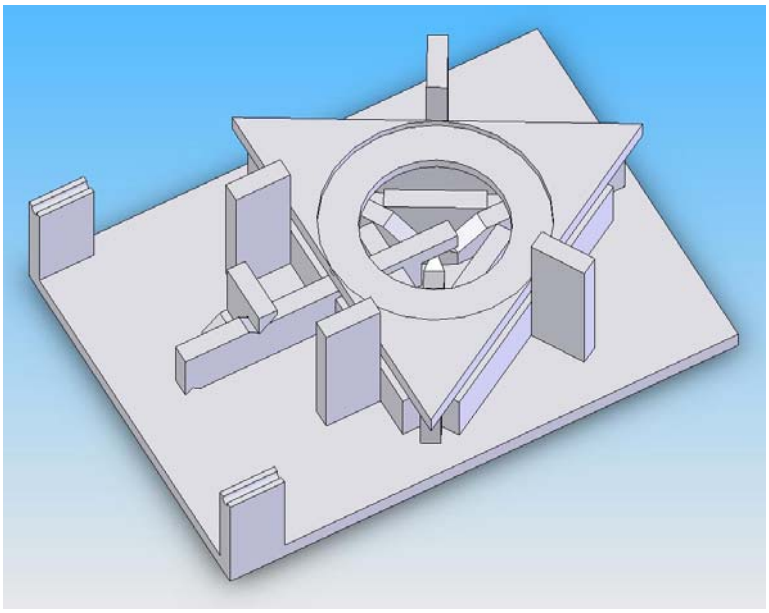

Figure A.4: Total WAT Device

The L1 levers have an ideal mechanical advantage (IMA) of 2, while the L2 lever has an IMA of 2.5; in series, the system has an IMA of 5. All four fulcrums are composed of an edge and notch, providing high energy transmission. The lever beams are designed to be level, so there are only y-components of the moments about the fulcrums. This also allows for virtually zero horizontal translation of the beam ends associated with minute rotations about the fulcrum, minimizing frictional energy loss at the contact points. The load cell data was to be recorded using data acquisition software and converted to a flow rate.

APPENDIX B

ACCULAB ALC SERIES SPEC SHEET

Model	ALC-80.4	ALC-110.4	ALC-210.4	ALC-150.3	ALC-320.3	ALC-810.2	ALC-1100.2	ALC-2100.2	ALC-3100.2	ALC-2100.1	ALC-4100.1	ALC-6100.1
Capacity	80 g	110 g	210 g	150 g	320 g	810 g	1100 g	2100 g	3100 g	2100 g	4100 g	6100 g
Readability	0.0001 g			0.001 g		0.01 g				0.1 g		
Tare Range (subtractive)	80 g	110 g	210 g	150 g	320 g	810 g	1100 g	2100 g	3100 g	2100 g	4100 g	6100 g
Repeatability	±0.1 mg			±1.5 mg	±1 mg	±0.01 g	±0.015 g	±0.01 g		±0.1 g		
Linearity	±0.3 mg			±2 mg		±0.02 g				±0.2 g		
Corner Load	±0.3 mg	±0.4 mg	±0.4 mg	±0.3 mg	±0.4 mg	±-.04 g				±0.4 g		
External Calibration Weight	50 g	100 g	200 g	100 g	200 g	500 g	1000 g	2000 g	2000 g	1000 g	2000 g	5000 g
Weighing Modes	grams, pounds, pounds/ounces, grains, parts/pound, milligrams, carats, pennyweight, troy ounces, Taiwanese taels, Hong Kong taels, Singapore taels, Chinese taels, mommes, Austrian carats, tola, baht, mesghal					grams, pounds, pounds/ounces, grains, parts/pound, milligrams, carats, pennyweight, troy ounces, Taiwanese taels, Hong Kong taels, Singapore taels, Chinese taels, mommes, Austrian carats, tola, baht, mesghal, kilograms						
Applications	mass unit conversion, counting, percentage weighing, averaging, plus weight unit toggle											
Display Type	LCD											
Audio Tone	at start up and function keys											
Overload Protection	yes											
Overload Indication	Displays "H"											
Underload Indication	Displays "L"											
Operating Humidity	less than 95% RH											
Operating Temperature	50° to 86°F (10° to 30°C)											
Allowable Ambient Operating Temperature	41° to 104°F (5° to 40°C)											
Stabilization Time (typical)	2.5 seconds			2 seconds						1.5 seconds		

Adaption to Ambient Operating Conditions	by selection of 1 of 4 optimized filter settings		
Display Update	0.2 to 0.8 seconds (depends on filter setting selected)		
Pan Size / Type	3.3" diameter (80 mm), stainless steel	6" diameter (150 mm), stainless steel	
Weighing Chamber Height	7.9" (200 mm)	n/a	
Dimensions	7.9 x 10.6 x 11.8 in (200 x 270 x 300 mm)	7.9 x 10.6 x 2.9 in (200 x 270 x 75 mm)	
DC Power Requirements	10-20V		
AC Power Requirements	AC adapter, 115V or 230V, +15%... -20%		
Frequency	48-60 Hz		
Power Consumption	1 watt (average)		0.75 watt (average)
Optional Accessories	calibration weights, RS232 interface cable		
Warranty	2 year manufacturer's warranty		

APPENDIX C

CACLULATIONS FOR REYNOLDS NUMBER AND THEORETICAL FLOW RATES

Reynolds Number

Reynolds number describes the ratio of inertial forces to viscous forces of fluid flow; determined by $R_e = \rho VD / \mu$, where the velocity was found for a nominal flow rate of 2.5 μL/min through the 0.076 cm diameter (D) tubing. The density (ρ) and dynamic viscosity (μ) values are for water.

Theoretical Flow Rate: Hagen- Poiseuille Equation

$$Q = (\pi D^4 \Delta p) / (128 \mu l)$$

where:
Q – flow rate
D – diameter of the tubing (0.076 cm)
Δp – hydrostatic pressure due to Δz
μ – dynamic viscosity (0.00112 Ns/m^2)
l – length of tubing (0.84 m)

REFERENCES

1. Bhattacharya, S. K.; Rockwood, E. J.; Smith, S. D.; Bonilha V. L.; Crabb, J. S.; Kuchtey, R. W.; Robertson, N. G.; Peachey, N. S.; Morton, C. C.; Crabb J. W. (2004). Proteomics Reveal Cochlin Deposits Associated with Glaucomatous Trabecular Meshwork. The Journal of Biological Chemistry, 280(7), 6080-6084.
2. Shade, D. L.; Clark, A. F.; Pang, I. H. (1996). Effects of Muscarinic Agents on Cultured Human Trabecular Meshwork Cells. Experimental Eye Research, 62, 201-210.
3. O'Brien, E. T.; Kinch, M.; Harding, T. W.; Epstein, D. L. (1997). A Mechanism for Trabecular Meshwork Cell Retraction: Ethacrynic Acid Initiates the Desphosphorylation of Focal Adhesion Proteins. Experimental Eye Research, 62, 201-210.
4. Markwardt, K. L.; Magnino, P. E.; Pang, I. H. (1997). Histamine Induced Contraction of Human Ciliary Muscle Cells. Experimental Eye Research, 64, 713-717.
5. Johnson, D. H.; Tschumper, R. C. (1987). Human Trabecular Meshwork Organ Culture: A New Method. Investigative Ophthalmology & Visual Science, 28(6), 945-953.
6. Johnson, D. H. (1996). Human Trabecular Meshwork Cell Survival is Dependent on Perfusion Rate. Investigative Ophthalmology & Visual Science, 37(6), 1204-1208.

7. Johnson, M. C.; Kamm, R. D. (1983). The Role of Schlemm's Canal in Aqueous Outflow from the Human Eye. Investigative Opthalmology & Visual Science, 24(3), 320-325.
8. MatWeb. Material Property Data. http://www.matweb.com/search/SpecificMaterial.asp?bassnum=PACPVC
9. Wikipedia. Eye. http://en.wikipedia.org/wiki/Eye

BIOGRAPHICAL INFORMATION

The author will now have an M.S. in Bioengineering to compliment his B.S. in Biological Engineering. He hopes to apply his expertise to industrial research and development, and possibly get his M.D. degree one day down the road.